Final Technical Report

Award Number: 04HQGR0166

REGIONAL WAVE PROPAGATION IN NEW ENGLAND AND NEW YORK: COLLABORATIVE RESEARCH WITH BOSTON UNIVERSITY AND TUFTS UNIVERSITY

Rachel E. Abercrombie
Department of Earth Sciences,
Boston University,
685 Commonwealth Avenue
Boston, MA 02215
Telephone: (617) 358-2571
Fax: (617) 353-3290
Email: rea@bu.edu

Laurie G. Baise
Department of Civil and Envir. Eng.
Tufts University
Anderson Hall
Medford, MA 02155 113
Telephone: (617) 627-2211
Fax: (617) 627-3994
Email: laurie.baise@tufts.edu

Program Element: Central and Eastern United States

Research supported by the U.S. Geological Survey (USGS). Department of the Interior, under USGS award number 04HQGR0166. The views and conclusions contained in this document are those of the authors and should not be interpreted as necessarily representing the official policies, either expressed or implied, of the U.S. Government.

Award Number: **04HQGR0166**

REGIONAL WAVE PROPAGATION IN NEW ENGLAND AND NEW YORK: COLLABORATIVE RESEARCH WITH BOSTON UNIVERSITY AND TUFTS UNIVERSITY

Rachel E. Abercrombie
Department of Earth Sciences,
Boston University,
685 Commonwealth Avenue
Boston, MA 02215
Telephone: (617) 358-2571
Fax: (617) 353-3290
Email: rea@bu.edu

Laurie G. Baise
Department of Civil and Environ. Eng.
Tufts University
Anderson Hall
Medford, MA 02155 113
Telephone: (617) 627-2211
Fax: (617) 627-3994
Email: laurie.baise@tufts.edu

Technical Abstract

To predict and mitigate the effects of future earthquakes in the northeastern United States, we need to know more about both the local earthquake sources, and how the seismic waves travel through the region. In this project, we investigate the source and regional wave propagation for the M5 20 April, 2002 Au Sable Forks earthquake. The Au Sable Forks earthquake is the largest earthquake in Eastern North America recorded at more than one good-quality broadband station. The Au Sable Forks epicenter is located near the boundary of two distinct geological provinces —Appalachian (New England) and Grenville (New York). We use the empirical Green's function method to determine the source time function that is then incorporated in the synthetic seismograms. We obtain a simple source pulse with an average duration of 1 second and corner frequency of 1 Hz. We estimate a static stress drop of 30 MPa, consistent with values expected for intraplate earthquakes. We then use a forward modeling approach for studying the waveforms, modeling data recorded at 16 stations located at less then 400 km of the epicenter. We generate synthetic seismograms using the frequency-wave number method. We test several published models for the two provinces. Several models perform well at low frequencies (<0.1 Hz).We choose as our preferred models, Saikia (1994) model 1 for the Appalachian Province and a model interpreted from a Hughes and Luetgert (1991) P-wave velocity cross-section for the Grenville Province. We refine these models, focusing on the upper layers, and generate two alternative one-dimensional (1D) crustal models for intermediate frequencies (<1 Hz). Our new Grenville model performs better at all of the 7 stations used than the published models. Our Appalachian model improves the fit of synthetics to data at 5 of the 10 stations used. The crustal models can be further constrained by incorporating specific site characteristics for each station, more detailed two-dimensional structure, and the observed anisotropy in the Appalachian province.

Award Number: **04HQGR0166**

REGIONAL WAVE PROPAGATION IN NEW ENGLAND AND NEW YORK: COLLABORATIVE RESEARCH WITH BOSTON UNIVERSITY AND TUFTS UNIVERSITY

Rachel E. Abercrombie
Department of Earth Sciences,
Boston University,
685 Commonwealth Avenue
Boston, MA 02215
Telephone: (617) 358-2571
Fax: (617) 353-3290
Email: rea@bu.edu

Laurie G. Baise
Department of Civil and Environ. Eng.
Tufts University
Anderson Hall
Medford, MA 02155 113
Telephone: (617) 627-2211
Fax: (617) 627-3994
Email: laurie.baise@tufts.edu

Non-Technical Abstract

To predict and mitigate the effects of future earthquakes in the northeastern United States, we need to know more about both the local earthquake sources, and how the seismic waves travel through the region. In this project, we investigate the source and regional wave propagation for the M5 20 April, 2002 Au Sable Forks earthquake. The Au Sable Forks earthquake is the largest earthquake in Eastern North America recorded at multiple good-quality broadband stations. The Au Sable Forks epicenter is located near the boundary of two distinct geological provinces —Appalachian (New England) and Grenville (New York). We test several existing one-dimensional (1D) crustal velocity models for each province which in general perform well at low frequencies. We then refine the preferred models to improve the fits at higher frequencies.

Introduction

We present a study of the source and the regional wave propagation of the Au Sable Forks earthquake (M_L5.3, M5.0, 20 April 2002). The Au Sable Forks earthquake is the largest earthquake to occur in the Northeastern United States since the installation of broadband networks in the region and so provides the first opportunity to investigate wave propagation at multiple stations and test regional models. The M5.9 Saguenay earthquake (25 November 1988) was the last moderate earthquake to have occurred in the region. It was recorded at one broadband station (HRV) and has had a significant influence on subsequent regional ground motion studies (Atkinson and Boore, 1995, 1998). The good-quality ground motions recorded during the Au Sable Forks earthquake at more than 50 modern broad-band stations provide a unique opportunity to investigate the source process, regional wave propagation, and ground motions of a moderate earthquake in the region. The earthquake was located near the Champlain Thrust that divides the Appalachian and the Grenville Provinces (see Figure 1). The differences in seismic wave velocities between the two provinces have long been established. The Proterozoic crust of the Grenville Province shows higher seismic velocities than the Paleozoic accreted terrains of the Appalachian Province (Musacchio et al., 1997). Because the Au Sable Forks earthquake epicenter is located near the boundary of the two provinces, we can use independent crustal models for each province. The Appalachian province is to the east of the epicenter and underlies New England whereas the Grenvillian province underlies New York State, west of the epicenter.

Atkinson and Sonley (2003) investigated the ground motions recorded by the Au Sable earthquake using a variety of spectral methods. They found that the earthquake ground motions are consistent with the prediction of several ground motion relations for eastern North America (Atkinson and Boore, 1995; Toro et al., 1997; Campbell, 2003; and Somerville et al., 2002). Hence they conclude that the Au Sable earthquake can be considered typical for an earthquake of this magnitude in Eastern North America. This research looks further into the source to better locate the aftershocks, determine the stress drop, and determine an appropriate source time function. Multiple one-dimensional velocity models exist in the literature for the two provinces (regional crustal models adopted by the LCSN network, Hughes and Luetgert (1991), Saikia (1994) and, Somerville (1989)); therefore, a goal of this research is to test and validate existing velocity models against the Au Sable Forks recorded ground motions. We use the frequency wave-number method and compare synthetic and recorded waveforms up to 1 Hz. In addition to the published one-dimensional velocity models, numerous reflection and refraction seismic analyses of the region (Hughes and Luetgert, 1991 and 1992; Hughes et al., 1993; Musacchio et al., 1997) provide additional information on crustal complexity. Therefore, an additional goal is to try to understand how crustal complexity affects the waveforms by performing sensitivity analysis and forward modeling iterations to incorporate crustal complexities.

Information on both earthquake sources and seismic energy propagation is fundamental to understand the possible effects of future moderate to large earthquakes in the Northeastern United States. This study provides important information on wave propagation and sources in the Northeastern United States for use in future seismic hazard work.

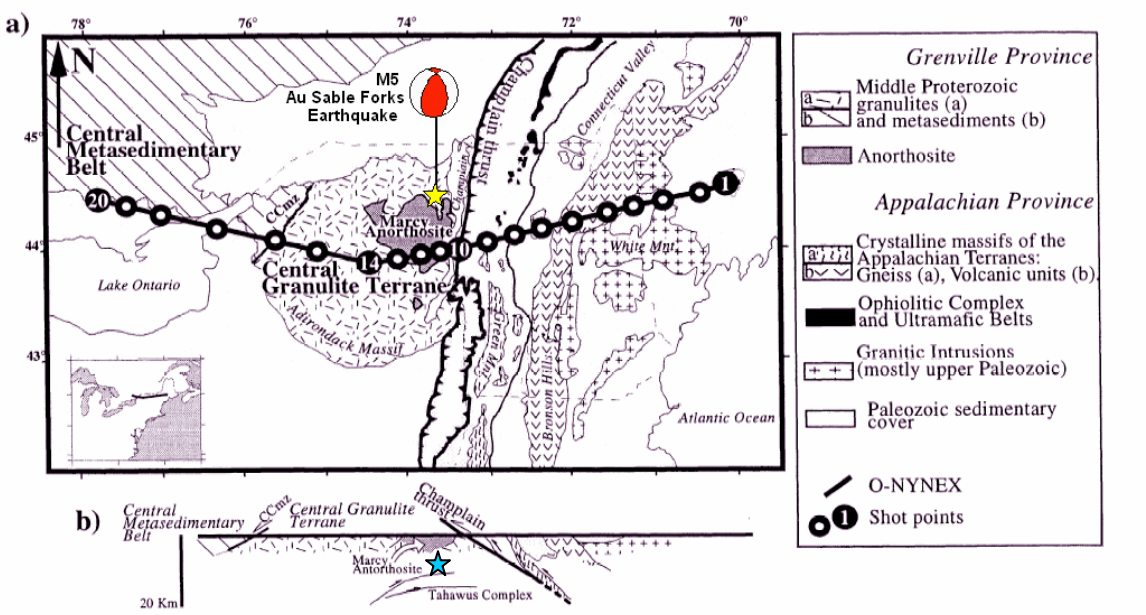

Figure 1. Geological map (a) and cross-section (b) of the Appalachian and Grenville Provinces. The Au Sable Forks focal mechanism, epicenter (yellow star) and hypocenter (blue star) are indicated on the map. The black circles indicate the shot points of the O-NYNEX Survey (Adapted from Mussachio et al. 1997).

Previous models for Eastern North America Earthquake Studies

Due to the low seismic activity of the region and the lack of large earthquakes, models of Eastern North America crustal structure rely on data from seismic surveys carried out since the 1950's (Eaton et al.,2006) for defining crustal properties. In 1988, the U.S. Geological Survey, the U.S. Air Force Geophysical Laboratory and the Geological Survey of Canada performed a large seismic survey that crossed the Appalachian and Grenville Provinces, the Ontario-New York–New England Seismic Refraction Profile (O-NYNEX). The refraction/wide-angle reflection survey (see Figure 1 for seismic profile) provided data for several studies. Hughes and Luetgert (1991) used a two-dimensional inversion technique to determine a seismic velocity model for the Grenville and Appalachian Provinces and Hughes and others (1993) further constrained the velocity models with seismic properties from sample rocks collected in the region and measured in the lab. Zhu and Ebel (1994) used a tomographic inversion technique to determine the velocity structures of Northern New England. Musacchio et al. (1997) used the P-wave to S-wave velocity ratio to determine the crustal composition of the two provinces. These studies show two common main features: a lateral velocity and Moho depth gradient, with higher velocities and greater Moho depths in the Grenville Province and slower velocities and smaller Moho depths in the Appalachian Province.

Ground motions from regional moderate earthquakes have also been used for crustal studies; however, previous studies relied on sparse seismic networks and limited data. Somerville (1989) derived a one dimensional (1D) velocity model for the Northern Appalachian province using aftershocks of the 1982 M5.6 New Brunswick earthquake.

More recently, Saikia (1994) refined an Appalachian 1D velocity model, by forward modeling broadband waveforms of the 1988 M5.9 Saguenay earthquake at station HRV.

The ground motion prediction equations built into the Probabilistic Seismic Hazard Analyses performed by the United States Geologic Survey for the Northeastern region of the United States rely heavily on simulations of ground motions using simple 1D crustal velocity models as do moment tensor inversion codes used to characterize sources in the region. Validation and updating of these models will therefore improve seismic hazard estimates for the region.

Geological setting

The Northeastern United States is characterized by two distinct lithologies. The Precambrian Grenville Province on the West, and the Paleozoic Appalachian Province on the East, that over thrust the Grenvillian basement (Seeber et al., 2002). The boundary between the two regions, the Taconic suture, is visible at the surface from the Labrador Sea to Alabama, and strikes approximately NNE-SSW (Wheeler, 1995). In New England, the boundary is expressed as the Champlain thrust, a 20 km deep East dipping fault (Musacchio et al., 1997) (Figure 1.b). Differences in crustal compositions of the two provinces reflect different formation processes and ages. Grenville autochthonous rocks are granulites and metasediments intruded by anorthosites, formed around 1 Ga ago during the Grenville orogeny (Hughes and Luetgert, 1992). The epicentral region is located on the east side of the Central Granulite Terrain (Adirondack Massif), close to a large anorthosite intrusion, to the West of the Champlain thrust. Appalachian rocks are younger and were formed during the complex Appalachian orogeny (500 Ma to 230 Ma ago), during the closing of the Iapetus ocean. It involved the accretion of two island arc terranes to the cratonic continent (Taconic and Acadian orogenies) and a posterior continental collision (Alleghanian orogeny) (Detweiler and Mooney, 2003). Appalachian rocks are mostly metasediments and gneissic and volcanic rocks intruded by granitic elements, formed during the mountain building episodes (Hughes and Luetgert, 1991). The different lithologies imprint different crustal properties.

Heat flow studies indicate that there is a sharp increase of about 15 mW/m^2 when transitioning from the Grenville Province to the Appalachian Province (e.g. Mareschal and Jaupart, 2004). Seismicity studies indicate that earthquakes occur at greater depths in the Grenville Province (e.g. Du et al., 2003; Ma and Atkinson, 2006). The large difference in heat flow values correlates well with differences in the seismicity depth range between the two provinces, indicating that the crust is thicker in the Grenville Province (Eaton et al., 2006). Attenuation of seismic waves varies within tectonic settings, reaching lower values for stable continental regions such as the cratonic Eastern North America (Frankel et al., 1990). Within the northeastern United States, regional attenuation studies (Shi et al., 1996) show that the Grenville Province has a higher crustal average quality factor Q than the Appalachian Province. The differences in attenuation also correlate well with the differences in crustal temperature, as waves are more attenuated when propagating through warmer media. In addition, studies of the regional crustal structure indicate that there is a difference in the propagation velocity of seismic waves between the two regions (e.g. Taylor et al., 1980; Musacchio et al., 1997; Hughes and Luetgert, 1991, 1992; Hughes et al., 1993), with the higher velocities in the Grenville

province being attributed to compositional differences (e.g. Musacchio et al., 1997; Hughes et al., 1993). In summary, Grenville crust is cooler and thicker and seismic waves propagate faster with less attenuation than in the Appalachian crust.

The Northeastern United States is characterized by low seismic activity, a typical feature of stable continental regions. The maximum compressive stress is fairly constant throughout the region. It is near-horizontal and trends to east-northeast on average (Du et al, 2003). The Au Sable forks earthquake occurred within the Appalachian seismogenic zone. The focal mechanism of the Au Sable Forks earthquake (see Figure 3) is consistent with the general trend of faulting in the region.

Data: The 2002 Au Sable Forks, NY, USA, Earthquake Sequence

The M5.0 earthquake occurred on April 20, 2002 near the town of Au Sable Forks, New York, USA. The earthquake epicenter was located at 44.51N latitude and 73.70W longitude and the estimated depth was 11 km (Seeber et al., 2002). This intraplate earthquake had a thrust mechanism with no surface rupture. It damaged roads, bridges, chimneys and water lines and was felt as far as Maine, Ohio, Michigan, Ontario and Maryland (USGS, 2002). It is the largest earthquake to be recorded by the 6 regional broadband networks installed within the last decade and the best recorded sequence in the Northeastern USA. It was recorded at more than 50 stations, at distances of 70 km to 2000 km (Figure 2). We limit our analysis to epicentral distances smaller than 400 km, significant for seismic hazard assessment, where the waveforms are simpler and have good signal to noise ratios. We analyze data recorded at 16 stations from 4 broadband networks: 3 stations (GAC, MNT and KGNO) from the Canadian National Seismograph Network (CNSN); 3 stations (BINY, LBNH, HRV) from the United States National Seismograph Network (USNSN); 3 stations (NCB, ACCN and CONY – seismograms at LSCT were cut) from the Lamont-Doherty Cooperative Seismographic Network (LCSN); and 7 stations (BCX, BRY, HNH, QUA2, WES, WVL and YLE – seismograms at stations VT1 and FFD were clipped) from New England Seismic Network (NESN). We integrate the velocity records to displacements, remove the instrument response and high pass filter above 0.01 Hz.

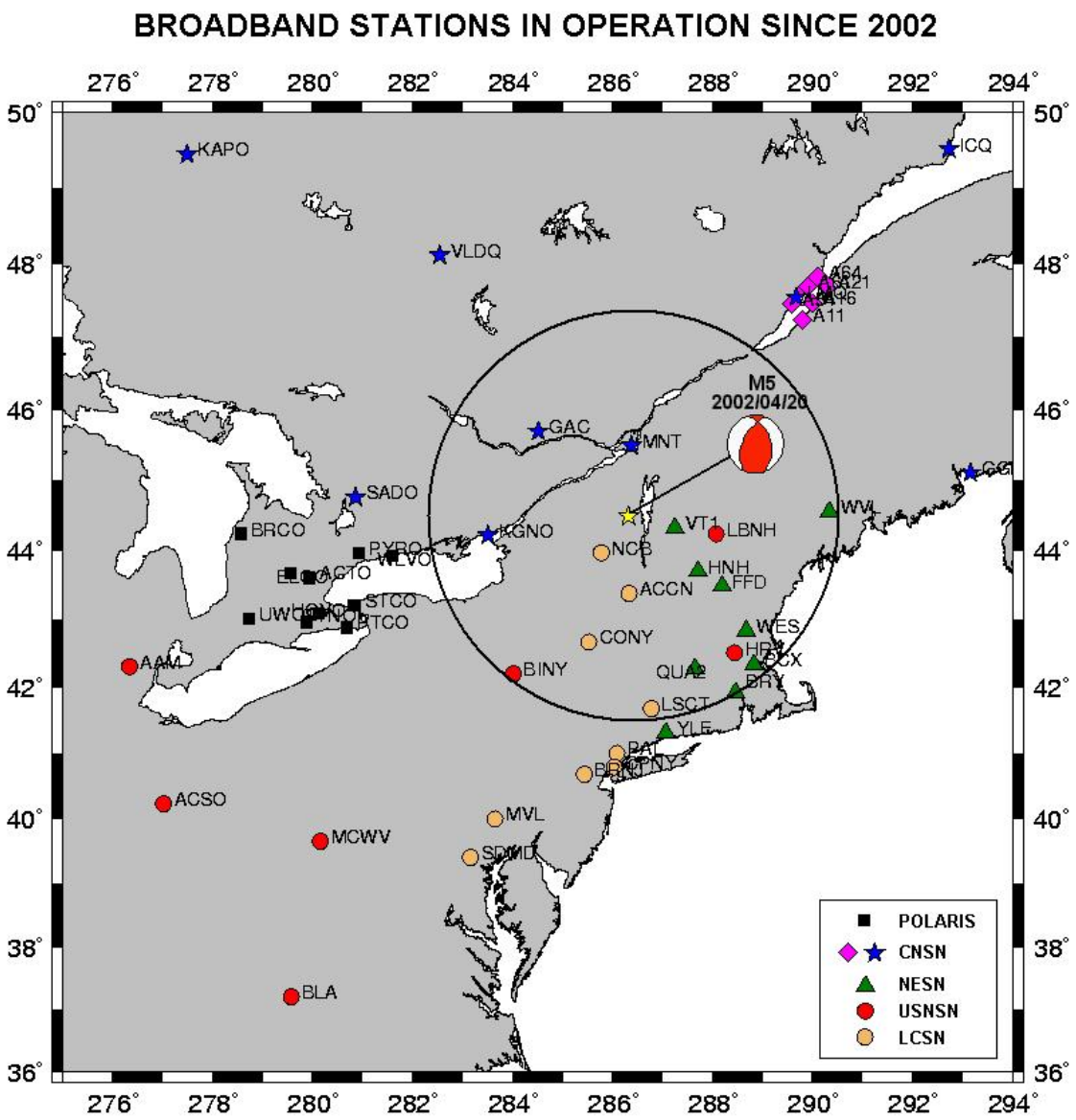

Figure 2. Broadband stations in operation on Eastern North America since 2002. Focal mechanism and epicenter (yellow star) of the 2002 Au Sable Fork earthquake. Circle constricts the stations used.

The Au Sable Forks earthquake had 9 aftershocks with local magnitudes between 3.7 and 2.2 (Table 1), large enough to be recorded by the broadband networks. All broadband data are available through the internet, except the NESN data that are available upon request, at the Weston Observatory in Weston, MA. The GSN/IRIS, USNSN, LCSN and CNSN broadband stations use a sampling rate of 40 sps and the NESN stations use a sampling rate of 100 sps.

Table 1. Au Sable Forks earthquake and largest aftershocks.

Number	Date (yyyy/mm/dd)	Time (hh:mm:ss)	Latitude (°)	Longitude (°)	Depth (km)	Magnitude (M_L)
1	4/20/2002	10:50:47.2	44.505	-73.669	12.5	5.3
2	4/20/2002	11:04:42.7	44.492	-73.679	13.4	3.7
3	4/20/2002	11:45:28.5	44.494	-73.684	11.3	2.9
4	4/21/2002	11:47:10.0	44.503	-73.645	10.6	2.2
5	4/21/2002	12:39:10.6	44.495	-73.680	11.8	2.3
6	4/25/2002	13:39:56.0	44.503	-73.679	11.1	2.2
7	5/24/2002	23:46:00.1	44.504	-73.669	12.0	3.1
8	5/25/2002	04:48:50.7	44.499	-73.669	11.6	2.4
9	6/25/2002	13:40:28.0	44.497	-73.669	10.9	3.0
10	12/25/2002	18:25:20.5	44.575	-73.765	11.4	2.4

Methods

We determine the source time function using the Empirical Green's Function (EGF) method (e.g. Hartzell, 1978; Abercrombie and Rice, 2005). The EGF method uses aftershocks as a transfer function representative of the medium the waves propagate through and the response of the instrument that records them. In order to be suitable for the EGF method, the aftershocks should comply with certain pre-requisites: it needs to have the same focal mechanism and location as the mainshock; and it needs to be one to two orders of magnitude smaller than the mainshock. We apply the EGF method to the nine aftershocks in the frequency domain and transform the result back to the time domain to obtain a source time function. Issues arising from the aftershocks not meeting the prerequisites are discussed below.

To calculate the stress drop we use the standard circular static crack solution (Eshelby, 1957). We assume Madariaga's (1976) source model to estimate the source dimension from our average source pulse duration and corner frequency.

We investigate wave propagation by forward-modeling the broadband records of the Au Sable Forks earthquake. We use a frequency wave-number code (e.g. Saikia, 1994) that computes Green's Functions for a layered crustal structure and generates preliminary synthetic seismograms. We model the Appalachian and Grenville Provinces records using 1D velocity crustal models characteristic of each province. We obtain final synthetics by convolving the preliminary synthetics with a source time function. The synthetics are compared to the data with absolute timing and amplitude unless otherwise stated.

Source

Seeber et al. (2002) and Won-Young Kim (personal communication, 2005) performed moment tensor inversions of regional broad-band recordings of the Au Sable Forks earthquake and its largest aftershock and obtained the respective source mechanisms, depths, and seismic moments, shown in Figure 3. Both earthquakes have thrust faulting mechanisms, but the P axis orientations are rotated by 100°. This difference in the focal mechanism trend can also be observed in the waveform shape,

namely in the P to S amplitude ratios. We compare the waveform shape of the mainshock (#1) and 9 largest aftershocks (Table 1) that were possible EGF earthquakes. All but the 25th Dec. aftershock (#10) have similar waveform shapes, indicating similar focal mechanisms, and are different from the mainshock (Figure 4). Further analysis of the 25th Dec. aftershock indicates this is a complex waveform composite of two small earthquakes, thus not suitable as an EGF. It is unfortunate and unusual that none of the largest aftershocks have the same focal mechanism as the mainshock.

Source Time Function

We apply the EGF method with each of the aftershocks, for both P and S regional waves. The best source time pulses are obtained with the largest aftershock (#2) as EGF for direct S waves. Figure 5 shows the best pulses obtained at seven stations. The degree of confidence on the source time function is limited by the discrepancies between the focal mechanisms of the two earthquakes (Seeber et al., 2002 and Won-Young Kim, personal comm., 2005). For the EGF method to work well, the radiation patterns have to coincide, otherwise, the amplitudes of various reflected and refracted phases will be incorrect in the EGF, leading to artificial complexity in the source time function. Still, the shape and duration of the obtained source-time functions are good enough to place constraints on the earthquake source. It has an average duration of about 1 second (40 samples) consistent with the duration obtained with the moment-tensor inversion (Seeber et al., 2002), and it is best described by a triangular simple pulse.

We use our average source pulse shape as input to the waveform modeling. We experiment using a single, triangular pulse (e.g. station LBNH in figure 5) and a double pulse (e.g. station CONY in Figure 5). We find that the single pulse fits the waveform best, implying that the STF complexity observed in the EGFs at some of the stations in Figure 5 results from uncertainties in the EGF deconvolution and does not reflect source complexity.

Due to the different focal mechanisms in the mainshock and aftershocks, we cannot determine directivity or sub-events. Any apparent directivity pattern or sub-events may be a consequence of different radiation patterns and not a source effect. For example, direct wave polarization may be different at the same station, altering the source pulse shape and duration when they are convolved. Thus, source complexity and apparent directivity are not reliable and we are unable to determine the fault plane, or to perform a slip inversion to determine the slip distribution on the fault plane.

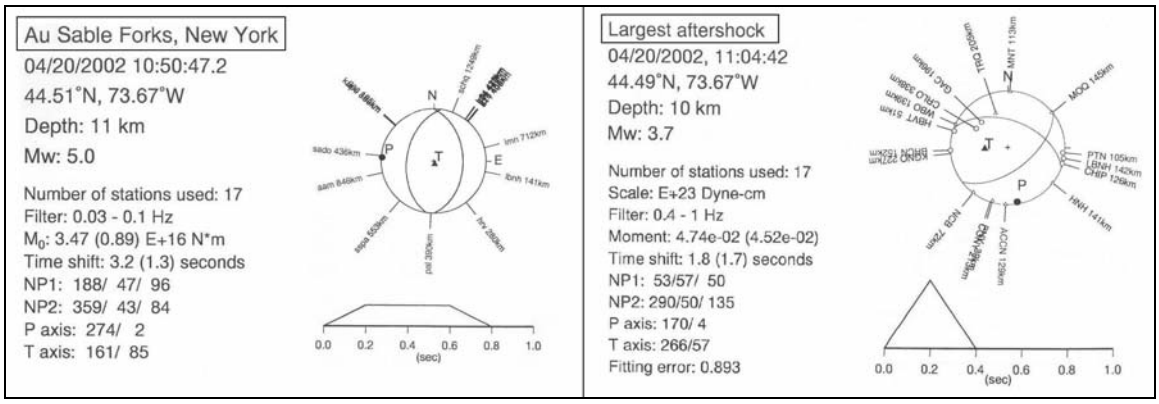

Figure 3. Source mechanism, depth, and moment of the Au Sable Forks earthquake and largest aftershock, determined by full wave modeling moment-tensor inversion of regional broadband seismograms (in Seeber et al., 2002 and Won-Young Kim, personal communication, 2005).

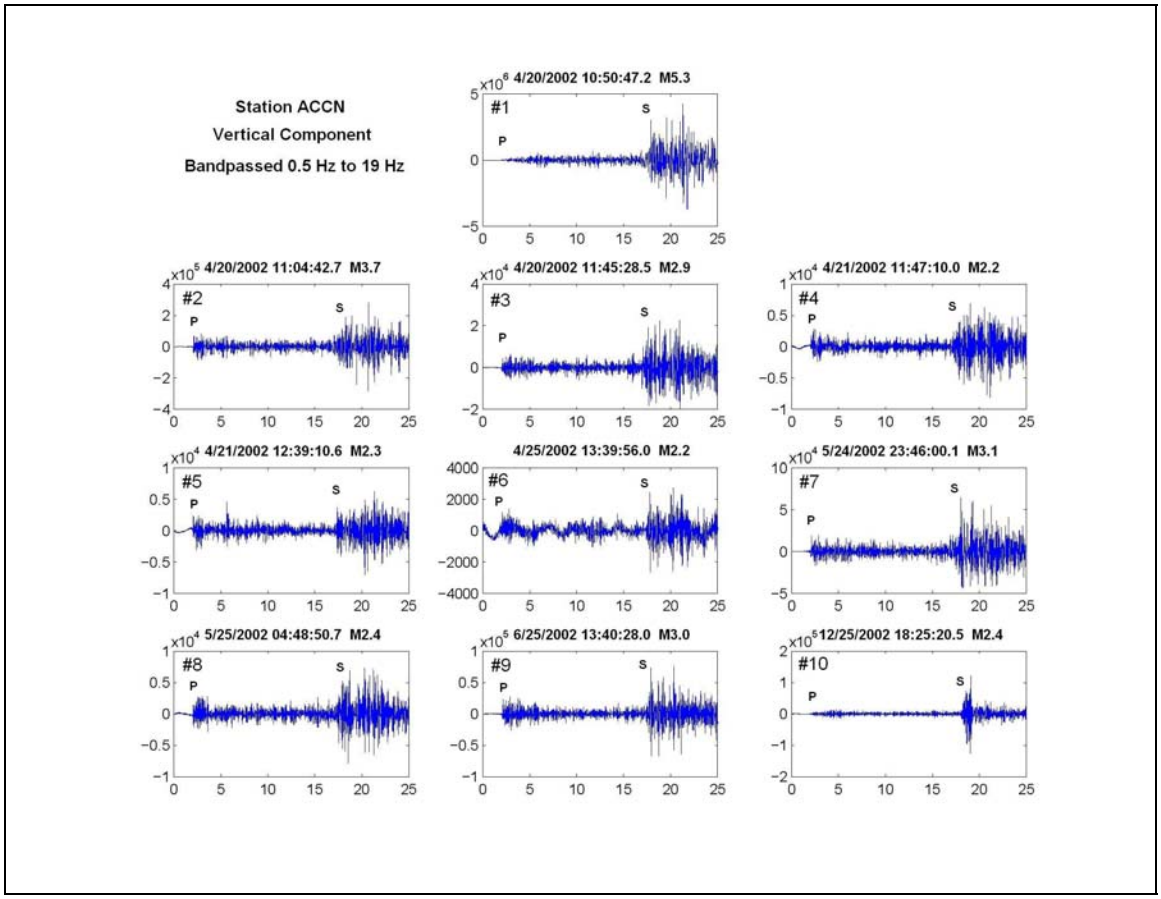

Figure 4. Vertical component of the mainshock (#1) and largest aftershocks (#2 to #10) velocity seismograms recorded at station ACCN. Seismograms are band-passed between 0.5 Hz and 19 Hz. Station ACCN is on a mainshock nodal plane. There is very little energy on the P wave when comparing with the S wave. The aftershocks show a higher P to S amplitude ratio, except for the 25th Dec aftershock (#10). Velocity units are nanometers per second and time units are seconds.

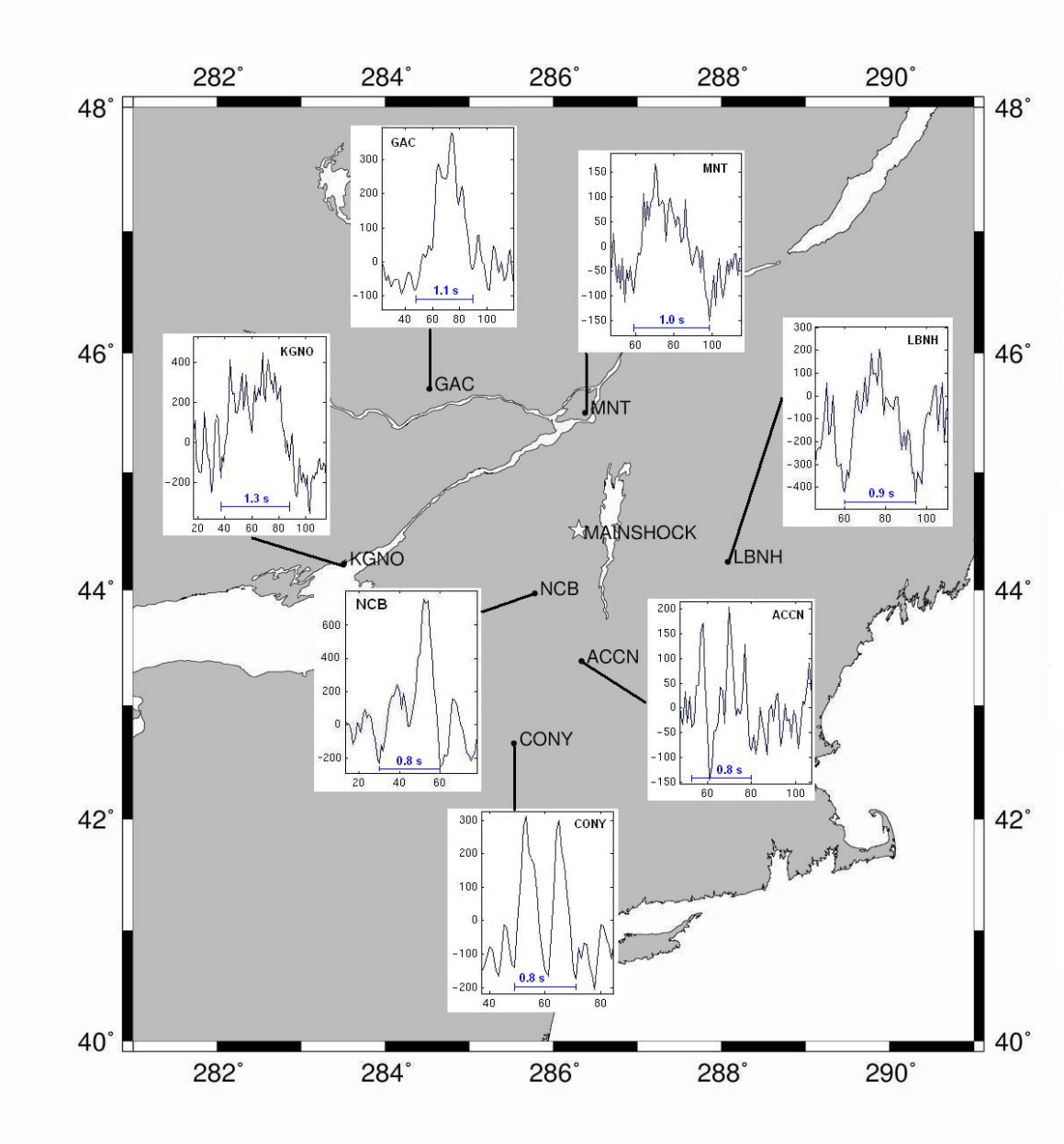

Figure 5. Best mainshock source-time pulses obtained at 7 stations, using largest aftershock as EGF, for regional recorded S waves.

Identifying Fault Plane

The EGF analysis does not provide a clear identification of the fault plane since we were unable to perform a slip inversion. We, therefore, look at the aftershock distribution to see if it illuminates the fault plane. In a parallel study, we (Kim and Abercrombie, 2006 and Viegas et al, 2005) relocated the mainshock and early aftershocks using a master event technique, and relocated the aftershocks recorded by a temporary local network using the double-difference method using differential travel times measured from waveform cross-correlation (Figure 6). The results show a systematic shift of epicentral locations to the east, consistent with the difference in propagation

velocity of the two provinces and the original 1D locations. A clear fault plane was not observed from the relocated aftershock distribution, indicating a complex conjugate sequence. We use the Seeber et al. (2002) nodal plane solution 1 (strike 188°, rake 96° and dip 47°. See NP1 in Figure 3) following the interpretation by Kim and Abercrombie (2006).

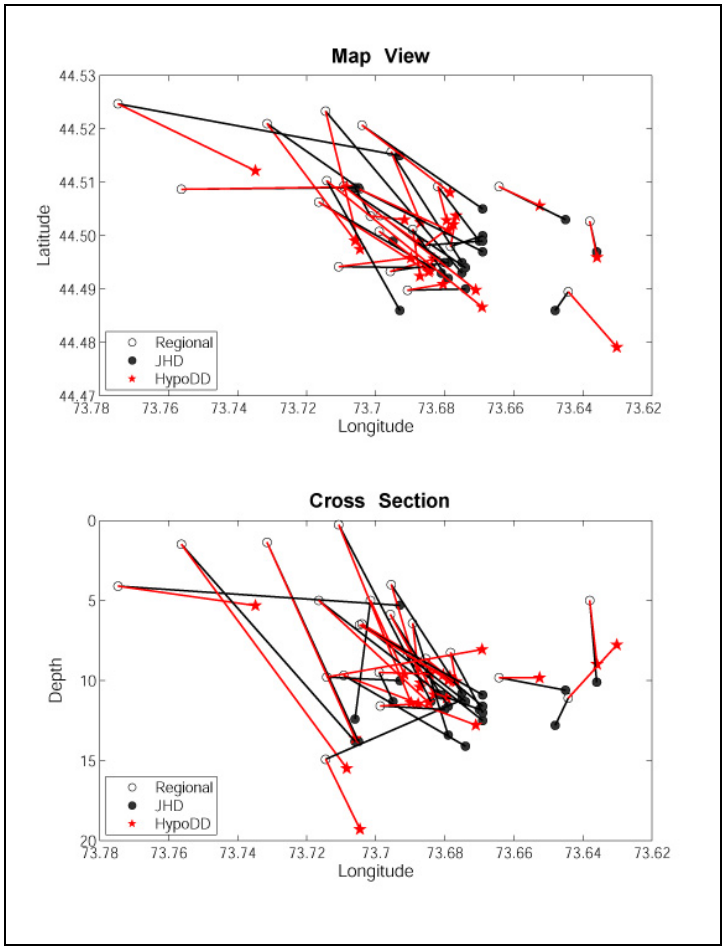

Figure 6. Map view (top) and cross-section (bottom) of the Au Sable Forks 2002 earthquake and largest aftershocks locations. Regional locations were calculated using a 1D regional model (open circles) and new locations using the Joint Hypocenter Determination method (black closed circles) and the Double-Difference method (red stars). Lines connect preliminary regional locations with new locations determined with the JHD method (black lines) or the HypoDD method (red lines).

Stress Drop

We can estimate an approximate stress drop from the average duration and corner frequency of our source pulses. We obtain a stress drop of 30 MPa, following Madariaga (1976) and Eshelby (1957), consistent with the idea that intraplate earthquakes have higher stress drops than those at plate boundaries, such as California earthquakes (Kanamori, 1975). Stress drop is an important source parameter as it is directly proportional to the ground acceleration.

Wave Propagation

Validation

Using published 1D crustal velocity models, we investigate wave propagation in the two provinces. We test the two regional crustal models adopted by the LCSN network for both provinces, the Hughes and Luetgert (1991) model for the Grenville Province, two crustal models from Saikia (1994) for the Appalachian Province, and the Somerville (1989) model also for the Appalachian Province. We use the attenuation — quality factor — and density values obtained by Saikia (1994) for the Appalachian Province and slightly decrease the attenuation for the Grenville Province, which is older and cooler. Figure 7 illustrates the 1D velocity profile of the above models for both P and S waves. LCSN models are simple three layer models. The surface layer is the main feature that distinguishes between the two regional LCSN models. It is thicker and slower in the Appalachian Province. The Grenville model (Hughes and Luetgert, 1991) is slightly faster than the LCSN one, and has a higher Moho depth. The Saikia (1994) models and Somerville (1989) model for the Appalachian Province are very complex, consisting of several layers. The main differences between the 3 models may be described by: an upper crust gradient (model 1 Saikia, 1994); alternated high and low thin velocity layers (model 2 Saikia, 1994); and a deeper Moho layer at 45 km of depth (Somerville, 1989).

The Grenville model (Hughes and Luetgert, 1991) was interpreted from a cross section figure, with indications of P wave velocities only. We built a velocity profile with depth based on the cross-section. Errors and uncertainties of depth measurements and estimated velocities are high. We construct the S wave profile using an initial average P wave to S wave velocity ratio of 1.73. We observe, on the synthetic seismograms generated with this model, that while P wave arrival times are good, S waves arrive too soon.

We generate synthetics using all the above models and pick one for each province that best fits the data at the most stations; thereby validating the 1D model across several paths. All waveforms are filtered to a bandpass of 0.03 Hz to 1 Hz unless otherwise specified. Figure 8 shows all Appalachian models simulated at the HRV station. The Saikia model 1 was developed specifically for the radial and vertical components of the HRV station; therefore, it is not surprising that the model synthetics are a good fit to the data for those components in both absolute timing and amplitudes of primary phases. The tangential component arrivals are later in the synthetics indicating possible anisotropy (discussed later). The LDEO and Saikia model 2 also fit the radial and vertical components of data well at HRV but have slight misfits in timing of primary phases. Saikia (1994) model 2 used alternated high and low thin velocity layers to create complexity at high frequencies, in order to better model the short period recordings at ETCN. This artifact, which does not have a physical expression in the crust, did not improve the synthetics in this study. The Somerville model does not perform well at the HRV station; the primary arrivals are significantly late indicating that the model is too slow and the synthetic amplitudes are too high. When comparing the synthetics to data at all nine stations in the Appalachian province, we found the Saikia (1994) model 1 to best fit the Au Sable Forks earthquake recorded waveforms. Figure 9 shows the synthetic waveforms compared to data for the vertical component at all nine stations in the Appalachian province for the Saikia model 1. The LDEO model, a simple three layered model performs well at low frequencies and is a good average model.

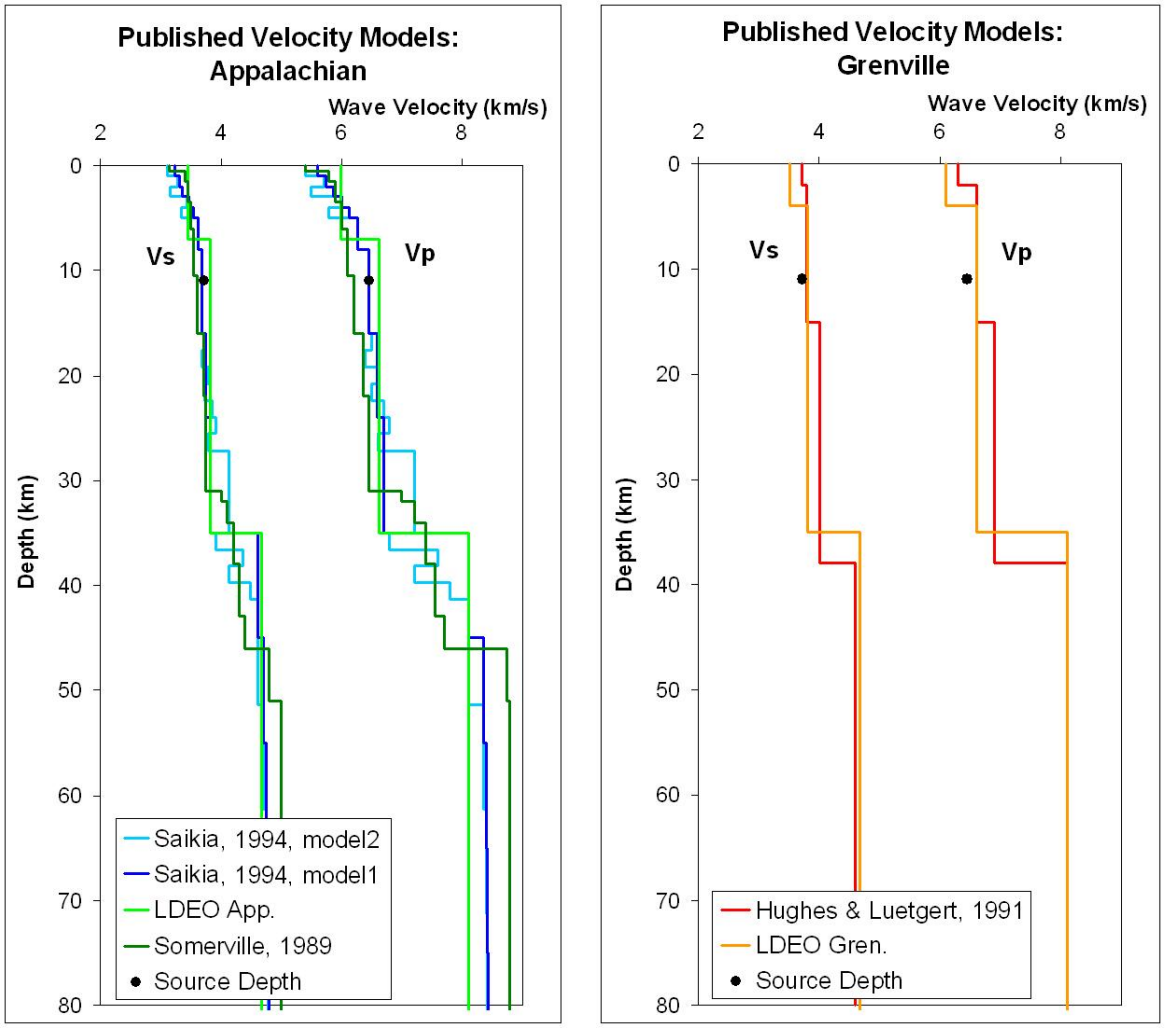

Figure 7. Published 1D velocity crustal models used in this study. **Left:** P and S wave velocity profile for the Appalachian Province (cold colors –slower velocities). **Right:** P and S wave velocity profile for the Grenville Province (warm colors –faster velocities). The mainshock depth is indicated by a black circle.

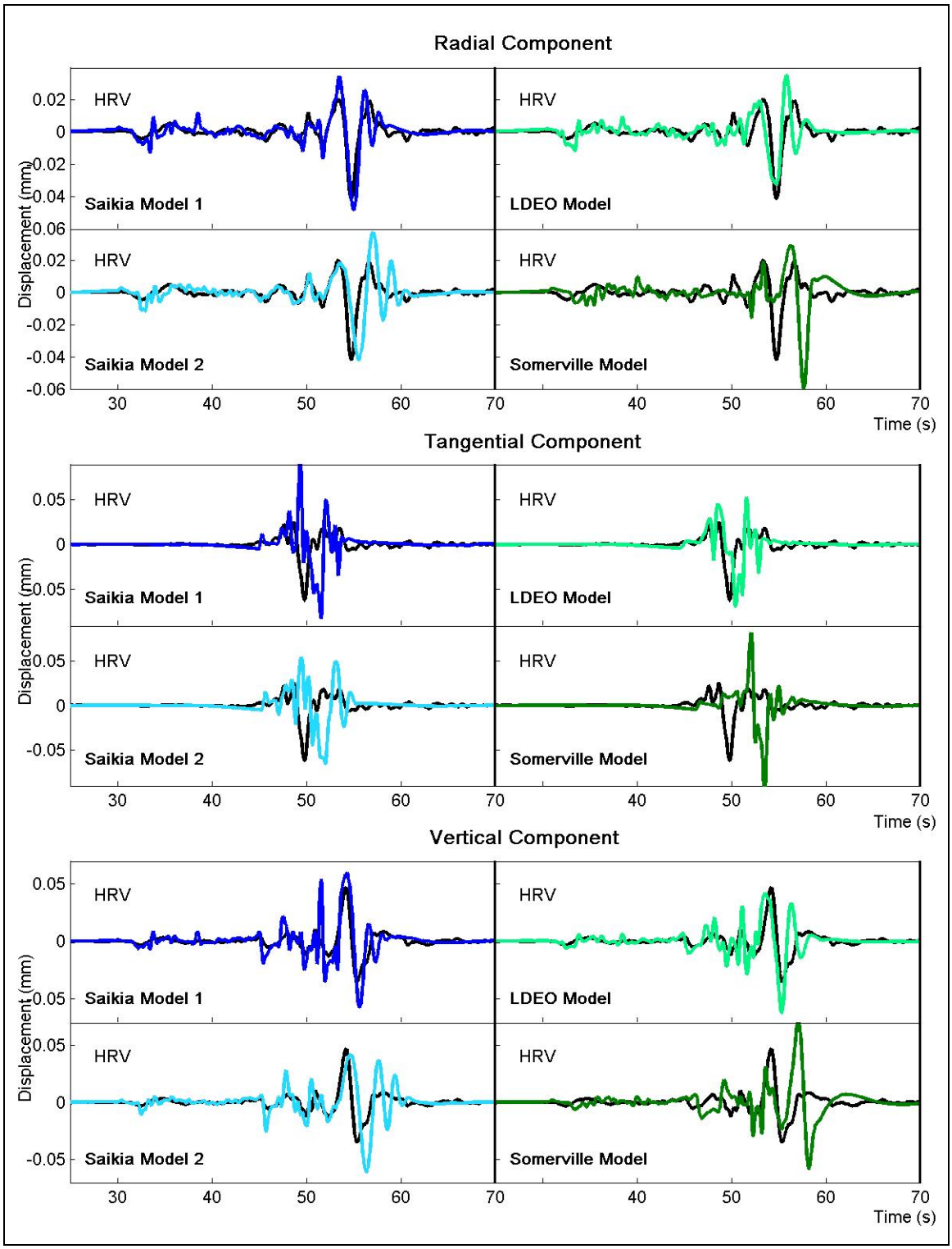

Figure 8. Synthetic displacement seismograms generated with 4 published crustal models for the Appalachian Province, at station HRV (Harvard, MA). Color code of Figure 7 is maintained (Saikia (1994) model 1 is blue; Saikia (1994) model 2 is cyan; LCNS model is light green; and Somerville (1989) model is dark green). Source is convolved in the synthetics. Seismograms are band passed between 0.03 Hz and 1 Hz.

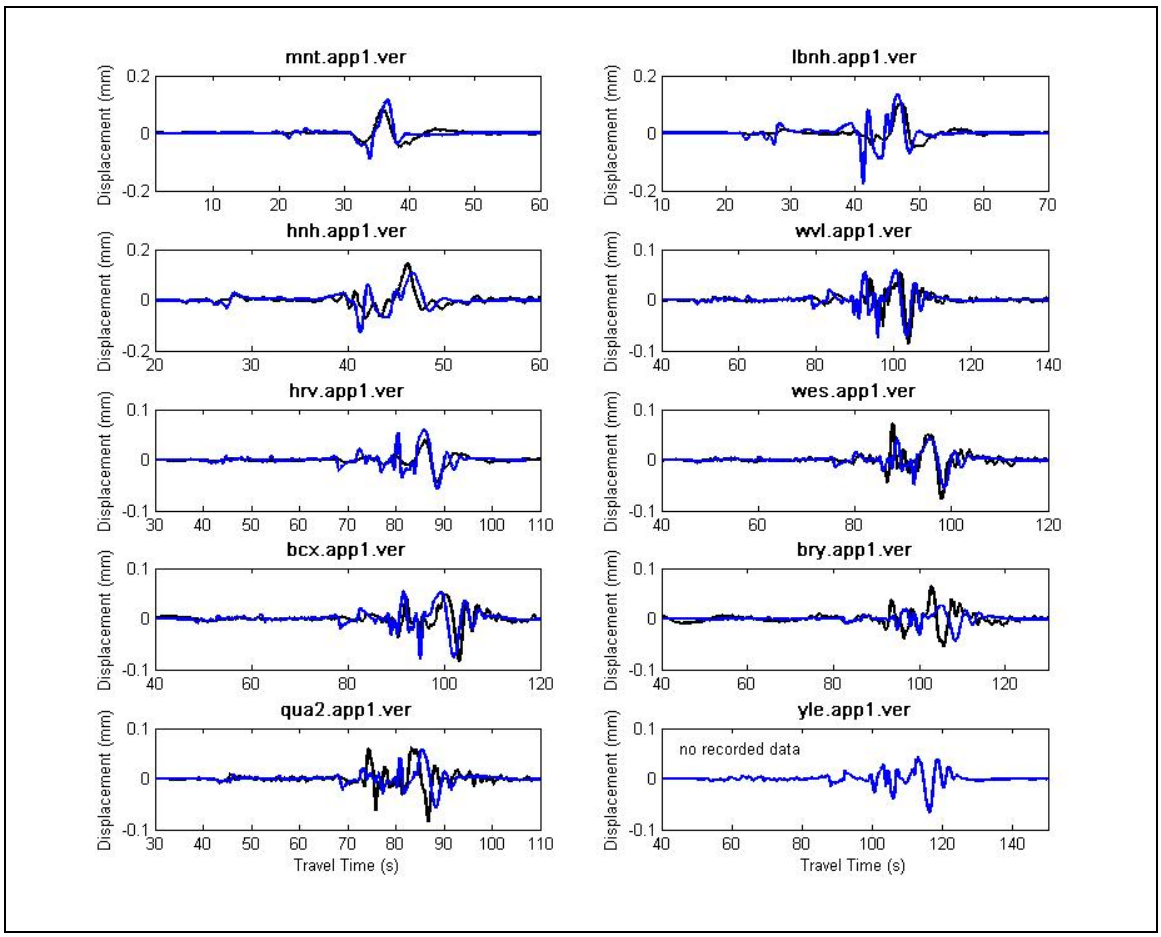

Figure 9. Recorded data (black) and synthetics generated with model App1 (blue) at stations within the Appalachian Province. Vertical component. All seismograms are band-passed between 0.03 Hz and 1 Hz. Source is convolved in the synthetics.

Figure 10 shows the Grenville models simulated at GAC. Neither model provides an excellent fit to the data. The timing of initial P-arrivals are modeled well on the radial and tangential components for both models and the timing and phasing of the later S-arrivals is better for the LDEO model. The LDEO model is a good average model; however, the layering does not match what has been observed in extensive study of the region (Hughes and Luetgert, 1991). After comparison across six stations in the Grenville province, we choose the Hughes and Luetgert (1991) model. Because neither model fit the data well initially, our choice was largely based on choosing a starting model that was consistent with regional crustal studies (including the greater Moho depth), although the LDEO model seem to better fit the later part of the recorded waveforms. As we will show later, this feature is achieved by a sharp velocity contrast between the two top layers and is incorporated into our final Grenville model. Figure 11 shows the Hughes and Luetgert (1991) model compared to data at the six stations in the Grenville province for the vertical component. As will be discussed in a later section, the S wave arrivals are too early for this model, indicating that our assumption of Vp/Vs ratio was too low. The

amplitude and phasing of the synthetics match the data and therefore the fits can be improved with a lower Vp/Vs ratio.

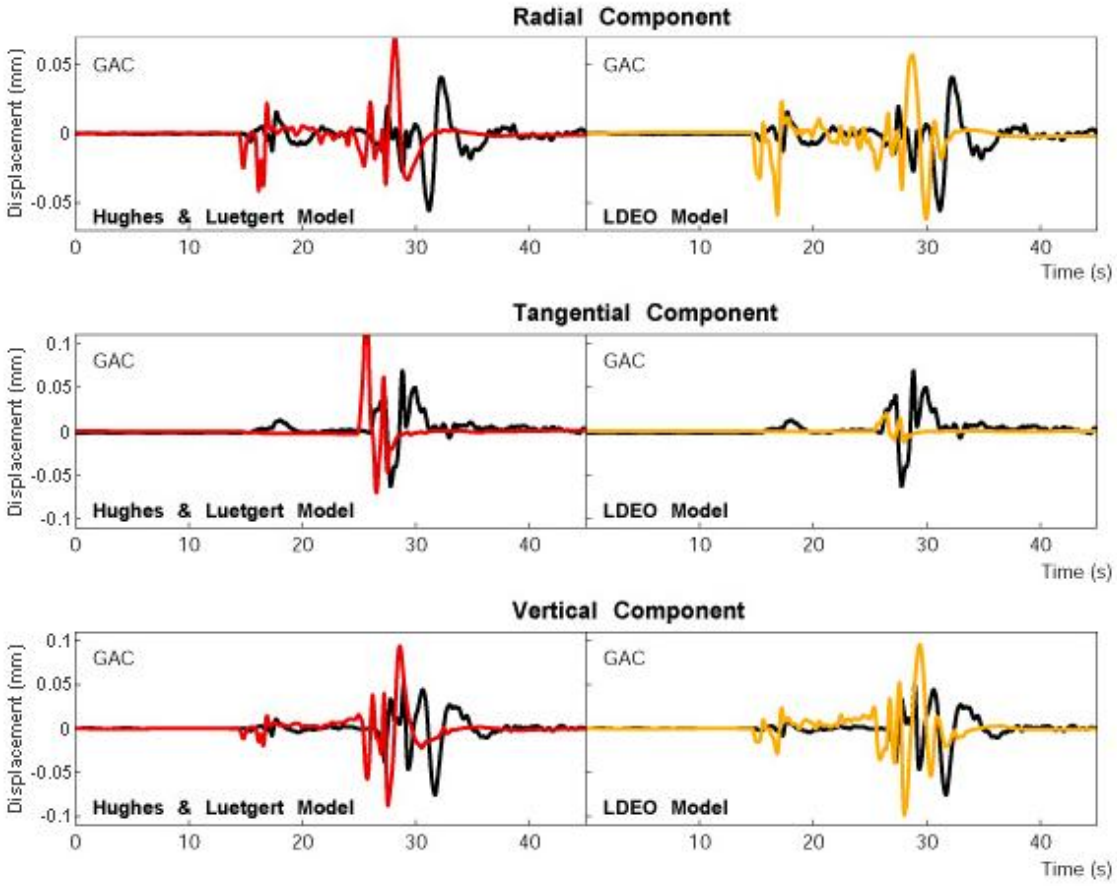

Figure 10. Synthetic displacement seismograms generated with 4 published crustal models for the Appalachian Province, at station GAC (Glen Almond, Quebec, Canada). Color code of Figure 7 is maintained (Hughes and Luetgert (1991) model is red; and LCNS model is dark yellow). Source is convolved in the synthetics. Seismograms are band passed between 0.03 Hz and 1 Hz.

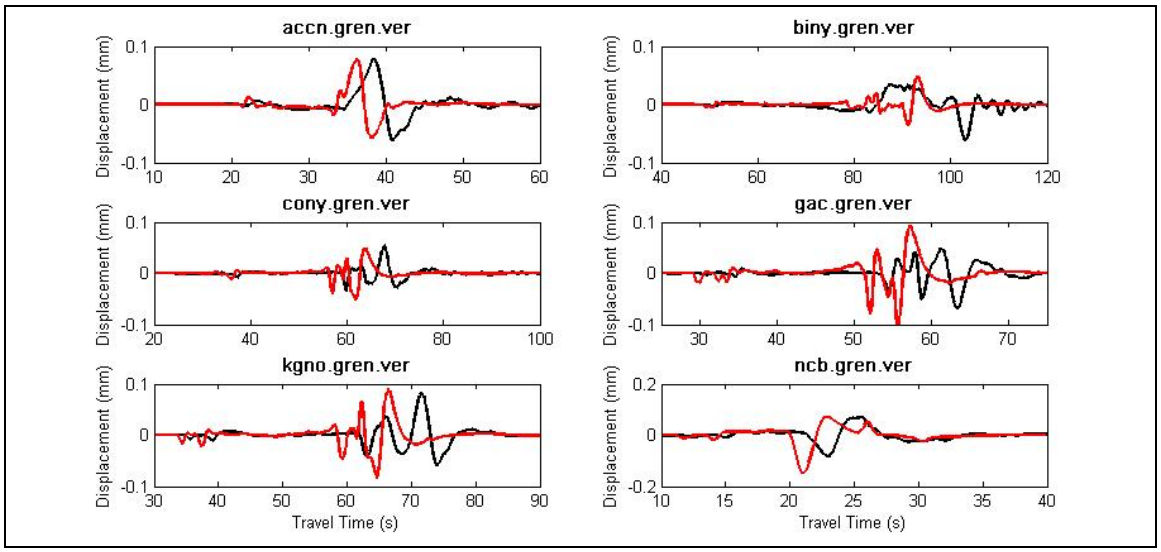

Figure 11. Recorded data (black) and synthetics generated with model Gren (red) at stations within the Grenville Province. Vertical component. All seismograms are band-passed between 0.03 Hz and 1 Hz. Source is convolved in the synthetics.

Sensitivity

Using the preferred models for each province, we perform two types of sensitivity tests. First we remove the layers one by one, to identify the contribution of each layer to the composite synthetic waveform, and second we vary the crustal model parameters, such as layer velocity or thickness, by increasing by small percentages, to determine the overall response of the waveform to these perturbations.

Removing the model layers gives us information on which boundaries or reflectors have a pronounced effect on the waveform shape. Figure 12 shows an example of the procedure applied to the Saikia (1994) model 1. The instrument-corrected displacement-seismogram recorded at station LBNH is displayed at the top. The preliminary synthetics are displayed in the lines below. The number of layers removed increases from top to bottom. Circles identify the wave arrivals suppressed when a layer is removed. In Figure 12, red circles indicate the multiple reflected waves suppressed by removing the Moho layer. The right side of the figure shows the P wave velocity profile and the how the gradual removal of layers is processed, starting from the deepest layers. The source time function is not convolved in this test because it smoothes the waveforms, making it more difficult to identify the wave arrivals.

The waveforms were not particularly sensitive to the slow increase in mantle velocity with depth. The upper layers contribute largely to the overall shape of the last part of the seismogram, as regional trapped waves and surfaces waves are the main constituent of the later part of the seismogram as seen in A14-A18. The interface at the base of the source layer contributes to the amplitude of the initial P as well as the early pS arrivals (A11-A12). The Moho reflector contributes with phases throughout the entire seismogram, as P and S waves reflect from this boundary.

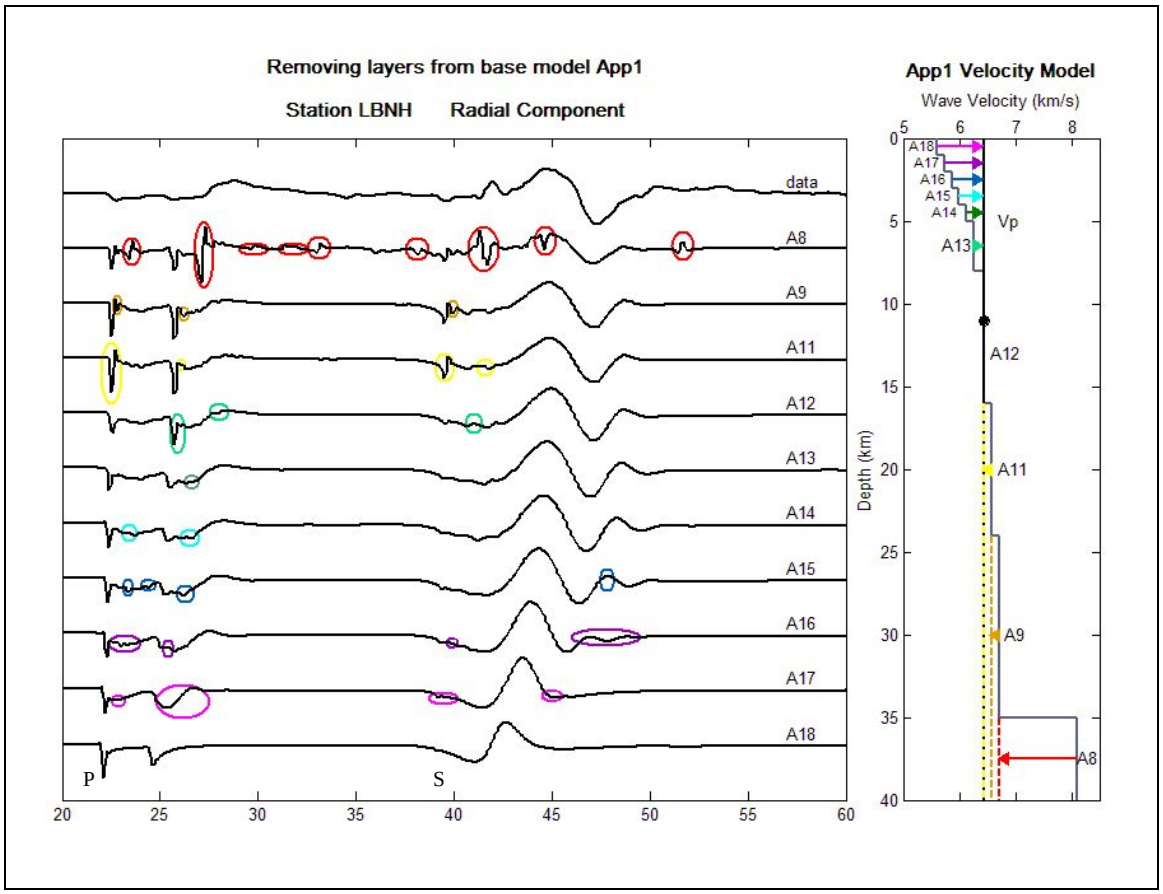

Figure 12. Removing layers. **Right side:** Saikia (1994) P wave velocity profile (grey) and intermediate profiles as layers are gradually removed, starting with the Moho layer (red) and ending with the surface layers. **Left side:** radial component of the instrument-corrected displacement seismogram recorded at station LBNH (top line) and preliminary synthetic seismograms generated with the intermediate profiles for station LBNH. Circles indicate suppressed arrivals.

Changing one or several layers properties, such as velocity or thickness, tells us how the full waveform responds to these changes, that is, how the wave arrivals change, relative to each other, to these perturbations. Our sensitivity analysis included a series of models perturbing the Moho depth, the intermediate layer velocities and thicknesses, and the upper layer (<5 km depth) structure (varying number of layers, as well as, velocities and thicknesses of layers). Figure 13 shows an example of velocity perturbations in model 1 from Saikia (1994) at LBNH. The sequence of models shown in the figure are tested to evaluate the sensitivity of the synthetics to increases in the velocity of intermediate crustal layers. By looking at the results over multiple stations, we find that the arrival times of certain phases were affected but that the overall fits of the models to data were not improved by increasing the velocity of the intermediate crustal layers. Figure 14 and 15 show waveform variation resulting from changes in the upper crust model for the Appalachian and Grenville Province models, respectively. The sensitivity analysis of the upper layers indicate that we can enhance late arrivals using either a

gradient or a sharp velocity contrast between the two upper layers with a thick surface layer (thicker than 3 km and 2 km for the Appalachian and Grenville Provinces, respectively). Based on this series of sensitivity tests combined with multi-station analysis, we identify the upper layers as the primary focus of our detailed modeling.

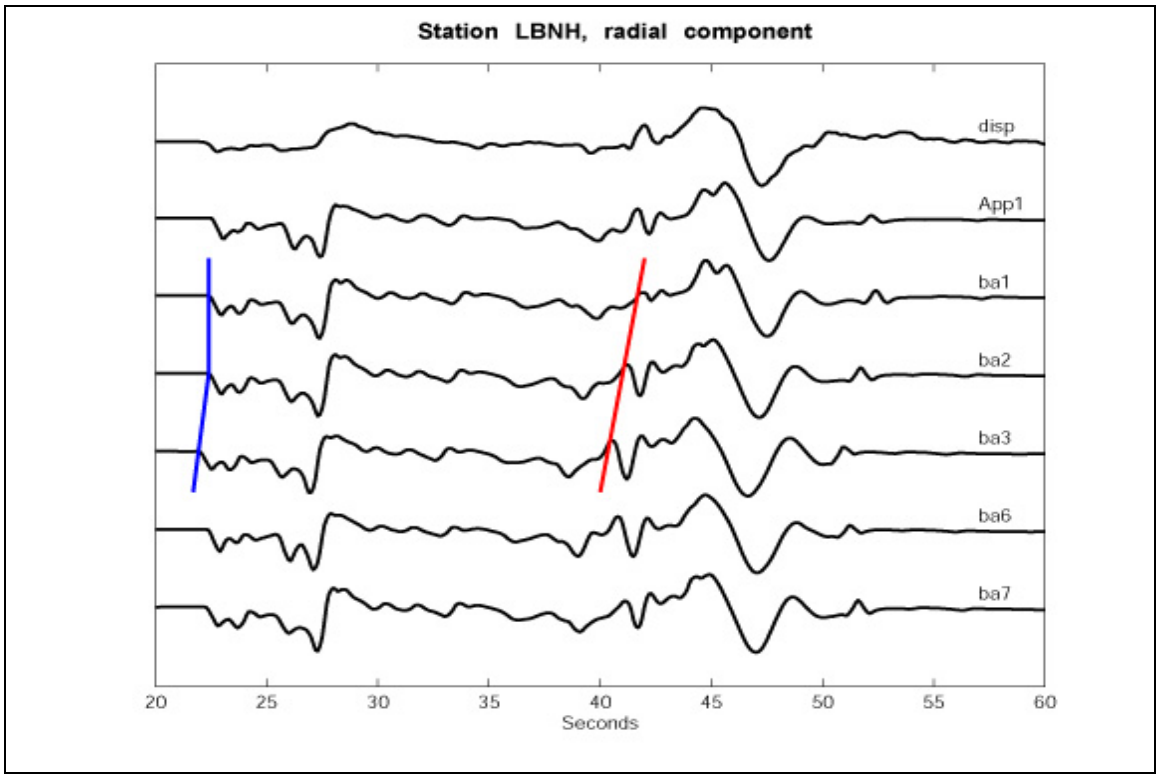

Figure 13. Perturbing velocities. Top seismogram is the displacement ground motion recorded at station LBNH (Lisbon, NH). Remaining seismograms are synthetics generated for that station with Saikia (1994) model 1 and derived models. Labeled models are (from top to bottom): **model App1** – Saikia model 1; **model ba1** – model App1 with one layer, instead of two, between the source and Moho layer; **model ba2** – model ba1 with Vp/Vs = 1.73 (increases Vs in the 2 lower crust layers); **model ba3** – model ba2 with faster source and down layers until Moho layer; **model ba6** – model ba2 with faster layer between source and Moho layers; **model ba7** – model ba2 with faster source layer. **Red line** indicates shape changes due to increase in S wave velocity in the intermediate and lower crust layers, anticipating the arrival of later phases. **Blue line** indicates the anticipation of the direct P wave arrival corresponding to the increase of the P wave velocity in the intermediate and lower crust layers from ba2 to ba3. The source is convolved in the synthetics.

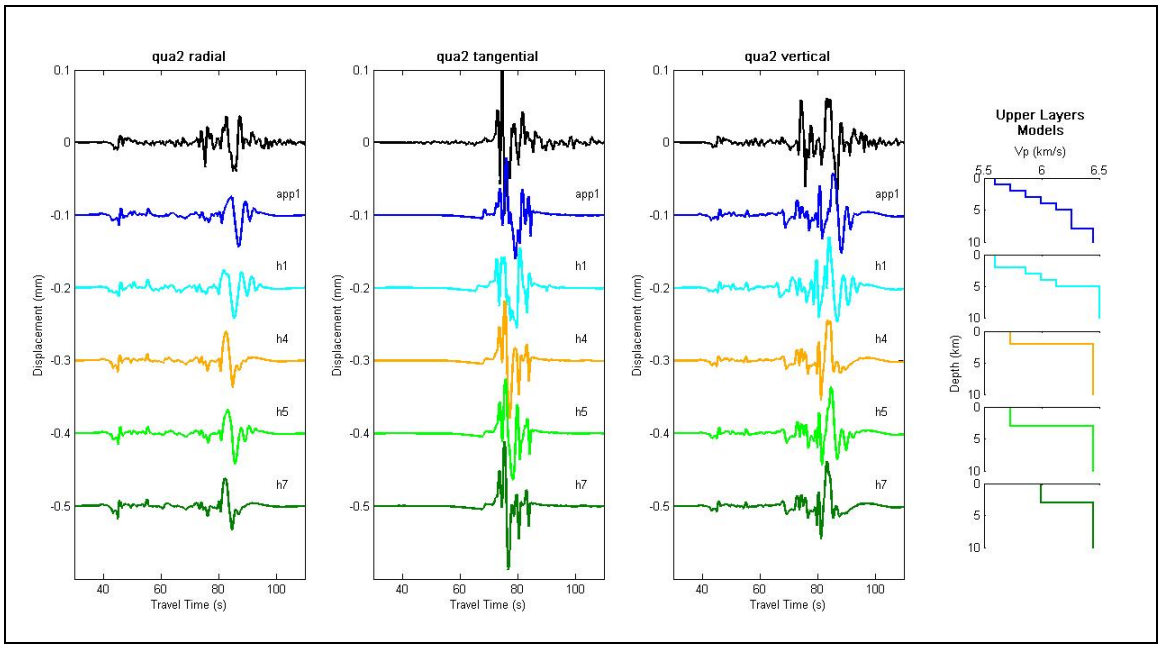

Figure 14. Changing the upper layers of Saikia (1994) model 1 (app1) at station QUA2. Black seismograms are the recorded data. Variations in the upper layers of the 1D velocity model are illustrated on the right side of the plot. Blue is the app1 model, cyan the h1 model, orange the h4 model, green the h5 model and dark green the h7 model. All three components are shown. Seismograms are band-passed between 0.03 Hz and 1 Hz and the source is convolved in the synthetics.

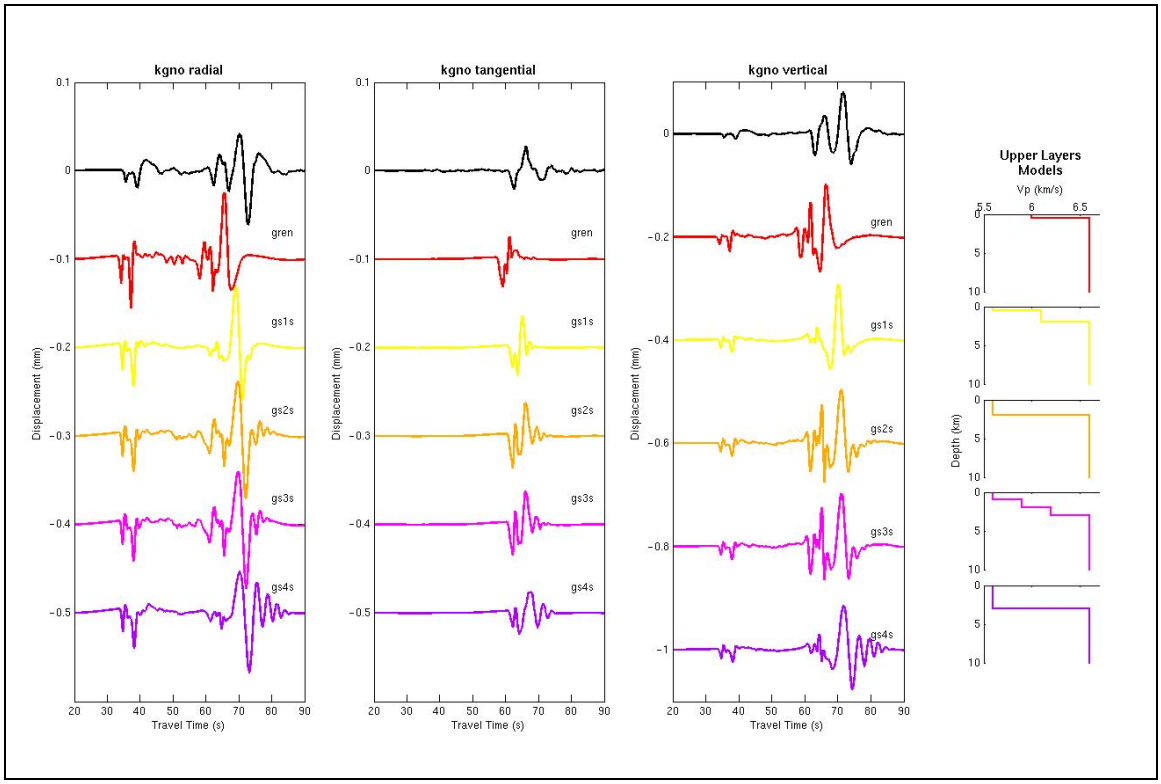

Figure 15. Changing the upper layers of Hughes and Luetgert (1991) model (gren) at station KGNO. Black seismograms are the recorded data. Variations in the upper layers of the 1D velocity model are illustrated on the right side of the plot. Red is the gren model, yellow the gs1s model, orange the gs2s model, magenta the gs3s model and purple the gs4s model. All three components are shown. Seismograms are band-passed between 0.03 Hz and 1 Hz and the source is convolved in the synthetics.

Focused Forward Modeling

Appalachian Province

For the Appalachian province, we choose Saikia (1994) model 1, hereafter called model App1, as the best published model (see Figure 9 above). It models the waveforms well, in terms of shape and arrival times of the main phases, for low frequencies (low passed at 0.1 Hz), at all the stations. Figure 16 shows the superposition of the 3 component recorded waveform and the synthetic waveform generated with model App1, low passed below 0.1 Hz, at station LBNH. We can therefore conclude that the main crustal layers are well identified in this model.

Model App1 is very detailed, including a velocity gradient in the first 5 km above the source layer that accounts for near surface effects at station HRV, for which it was developed. At other stations, the upper crust structure may be different. From our sensitivity analysis, we find that the waveforms were sensitive to the upper crust structure and that perturbations to this structure could improve the waveform fits. We develop

several combinations of upper crust layers, maintaining the intermediate and lower crust profile. We try one to three surface layers, with different thicknesses and velocity contrasts. We keep the P wave to S wave velocity ratio equal to 1.73, consistent with values obtained by Musacchio et al. (1997) in a regional study of ENA crust composition. We expect the results to differ by station, however, the original surface layers in App1 and one other model with a single 3 km deep surface layer provide the best fits for all of the stations in the Appalachian province. An example of the improved fit is shown in Figure 17 for station QUA2, where the superposition of the recorded and synthetics waveforms is shown for both App1 and h5 models. In Figure 18 we graphically depict the 1D velocity profile of model App1 and, in the inset, the change in the surface layers introduced by our new model h5. Plots of the synthetics resulting from the preferred models versus the data at each station in the Appalachian province can be found in the Appendix.

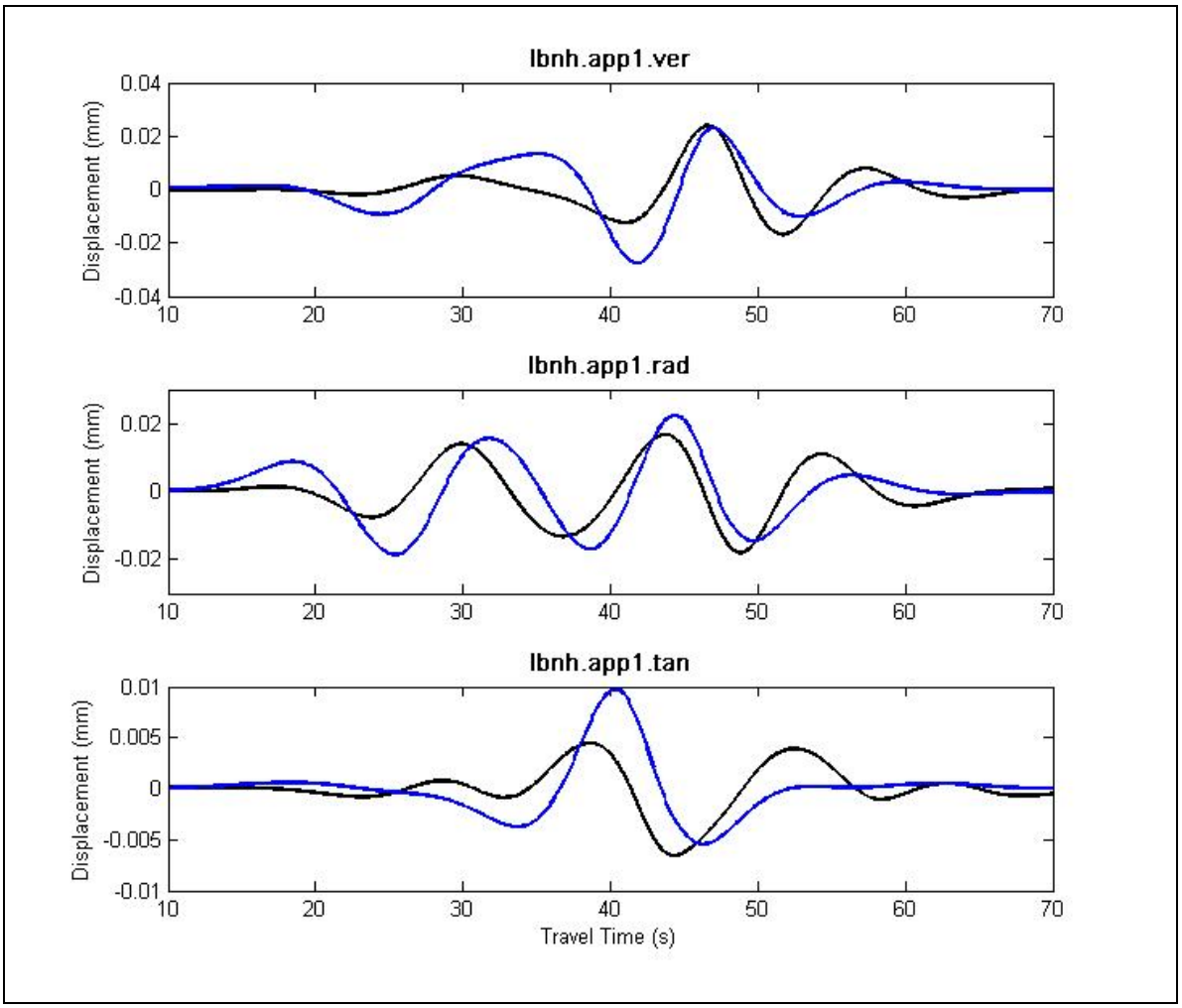

Figure 16. Recorded waveform (black line) and synthetic waveform (blue line) generated with model App1, at station LBNH (Lisbon, NH, USA), low passed below 0.1 Hz.

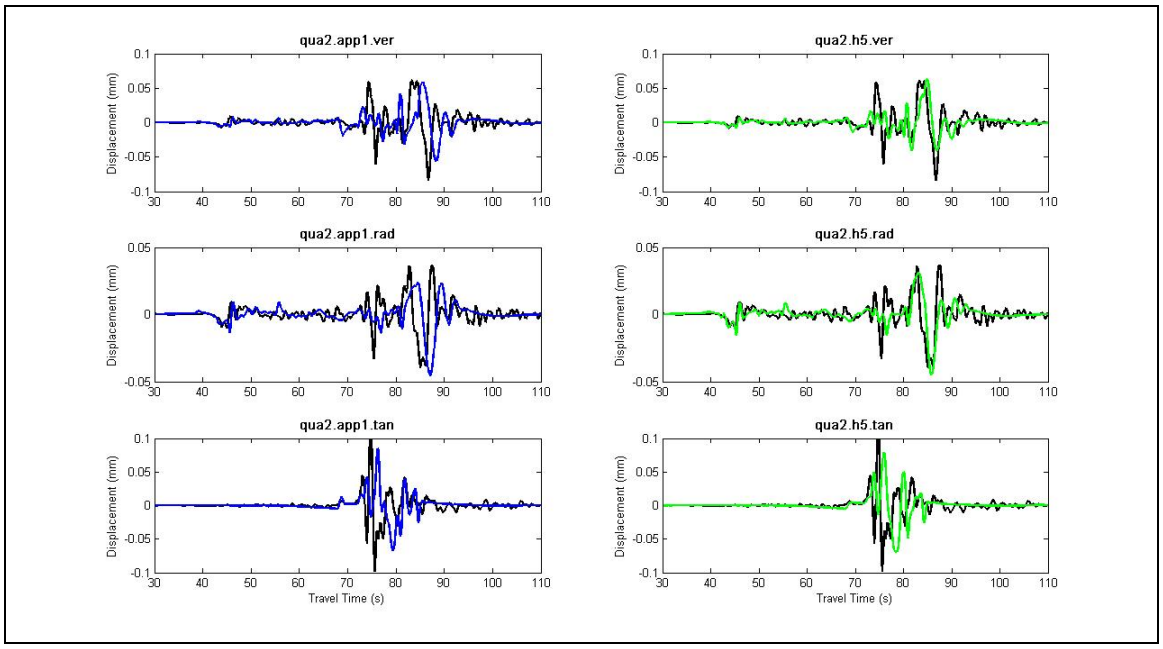

Figure 17. Superposition of three component recorded waveform (black line) with synthetics generated with model App1 (left, blue line) and generated with model h5 (right, green line), at station QUA2 (Belchertown, MA). The waveforms are low passed filtered to 1 Hz.

Anisotropy in the Appalachian Province

The tangential component at station HRV shows a 3 s shift of S wave arrival time, with the data arriving before the synthetic. This shift is not seen on the other two components, vertical and radial. All three component waveforms are aligned by Event Origin Time (EOT). This implies that SH is slightly faster than SV. The App1 velocity model was developed by Saikia (1994), but only radial and vertical components were fitted. Saikia (1994) refined a pre-existing model from Zhao and Helmberger (1991), which modeled the 3 component broadband waveforms of the 1988 M5.9 Saguenay earthquake at station HRV. Zhao and Helmberger (1991) also observed a time shift for the tangential component of 1.5 seconds. They proposed as possible mechanisms epicentral distance uncertainty or anisotropy due to shear wave splitting or a regional anomaly. We notice that this feature is also observed at nearby stations, with similar azimuths and epicentral distances (Figure 19). The shift of S arrivals varies from 1.0 s (QUA2 – 270 km) to 3.0 s (WES – 303 km) indicating a significant and consistent delay that is not directly proportional to epicentral distance. QUA2 which has the smallest shift is 70 km east of HRV. Hughes et al. (1993) identified a series of steep dipping reflectors beneath the Green Mountains in Southern Vermont, characterized by 2 % to 12 % seismic anisotropy. They interpreted it as foliated gneisses with highly anisotropic minerals that show a preferential alignment direction. These paragneisses may be responsible for an increase in seismic velocity of waves propagating parallel to the foliation and for a decrease in seismic velocity of waves propagating normal to the foliation (Figure 20). A time shift of 2.5 seconds is too large to result solely from shear wave splitting in a 10 km thick near-vertical layer with 10 % anisotropy. The wave path

for these stations is near parallel/low angle to the Green Mountain Belt and can account for a longer propagation within the anisotropic medium. The boundary zone between the two provinces is an old suture with deeply imbricated structures below and to the East of the Green Mountains (see Figure 21). Anisotropy can also be caused by preferential stratification and fracture orientation.

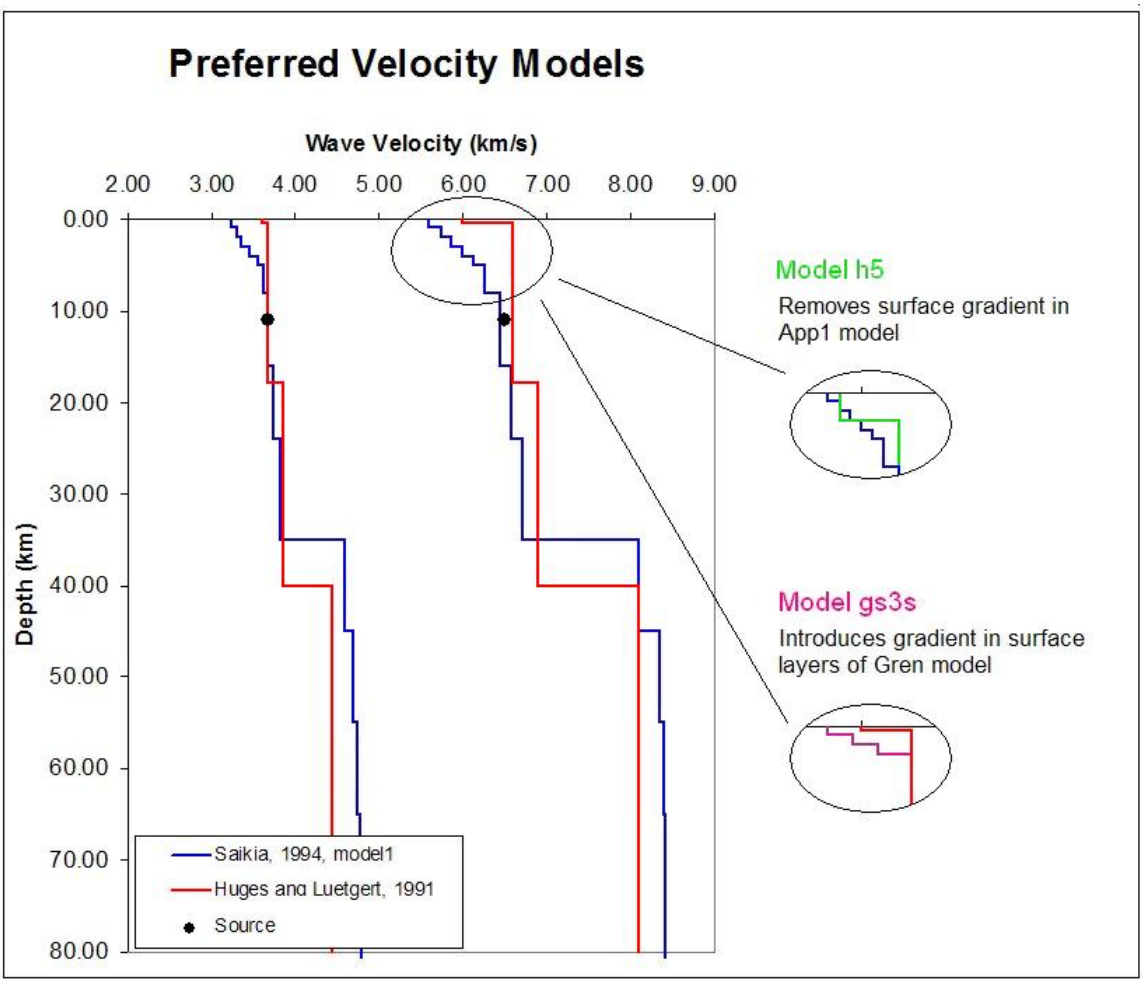

Figure 18. Initial Grenville (red) and Appalachian (blue) 1D crustal seismic velocity model, for the Au Sable Forks Earthquake. Insets indicate changes in the upper crust layers introduced in this study: model h5 replaces a 5 layer gradient (blue) with 1 surface layer with a large velocity contrast (green), and model gs3s introduces a three layer gradient in the upper crust (magenta) instead of a shallow high velocity surface layer (red).

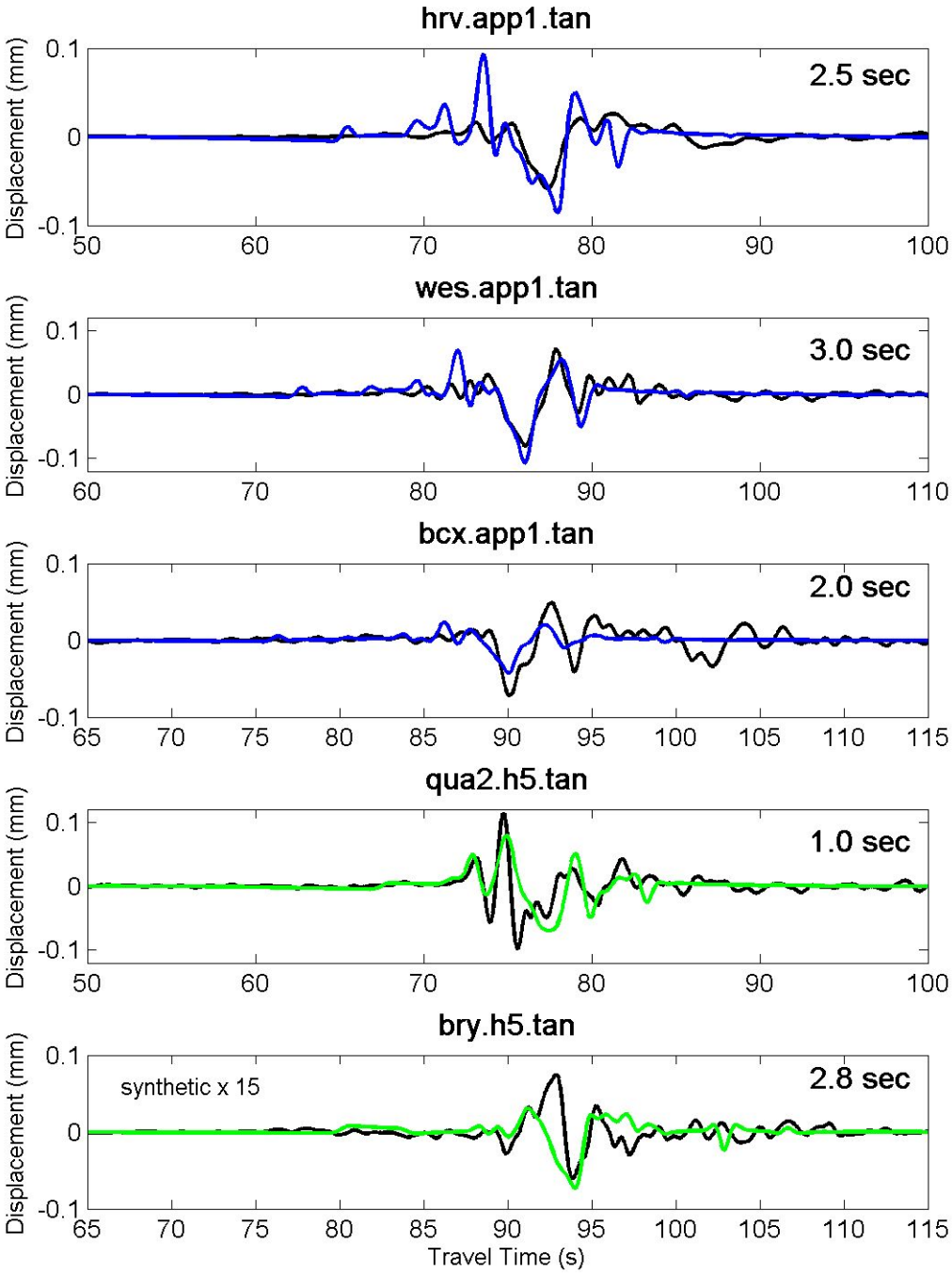

Figure 19. Anisotropy.Tangential component at stations QUA2, WES, HRV, BCX and BRY. Black line is the recorded data and colored line the synthetics. Numbers on the top right corner represents the time interval the synthetics are shifted. BRY synthetic was multiplied by 15 to better compare with recorded data at that station.

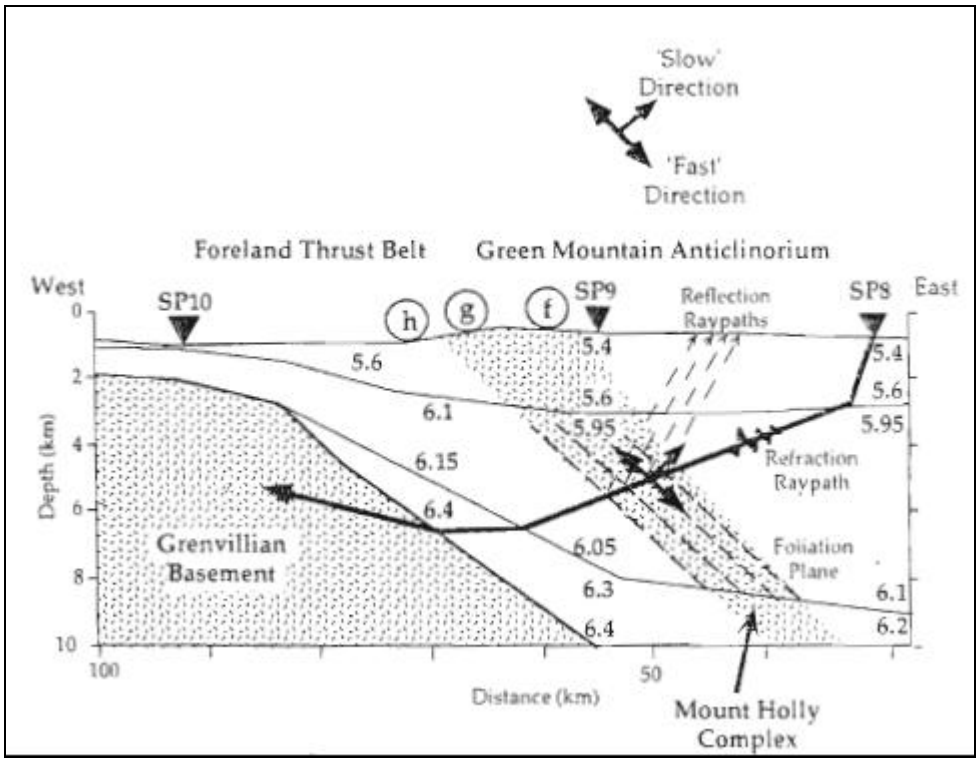

Figure 20. Cross section from Hughes et al. 1993 showing foliation plane of mylonitized gneisses of the Green Montain Anticlinorium. The Gneisses are characterized by 5 % anisotropy. Fast and slow directions are indicated. See Figure 1 or 21 for shoot point 10 (SP10) location.

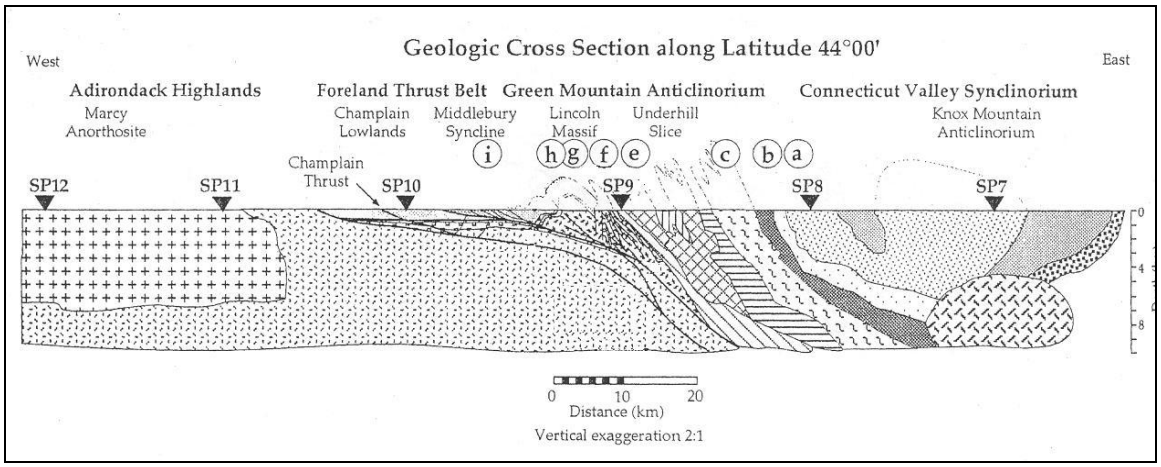

Figure 21. Geologic cross section along the Ontario – New York – New England regions at latitude 44 N, showing the dipping imbricated structures at the edge of the Grenvillian crust. (Adapted from Hughes et al. 1993).

Grenville Province

We choose the model derived from the Hughes and Luetgert (1991) P-wave velocity cross-section, hereafter called model Gren, as the best published model (see Figure 11 above). In the validation tests, the S wave arrivals were early indicating that

our assumption for defining S wave velocities (that the Vp/Vs ratio was the same as defined for the Appalachian province) was flawed. We correct the S waves arrival times by decreasing the S wave velocities within all layers. We obtain a good fit with an average P wave to S wave velocity ratio of 1.80. This value is consistent with the Musacchio et al. (1997) study of the crustal composition in the Grenville Province and with the Eaton et al. (2006) study of Vp/Vs variations in the Grenville Orogen. The different ratio reveals the differences in the crust composition of the two provinces. When comparing the velocity profiles of both regions, we observe that the higher ratio is a result of a higher P wave velocity, whereas the S wave velocities are approximately the same in the two provinces. This indicates that the differences in the Vp/Vs ratio do not come from higher water content in the Grenville province, that would lower the shear wave propagation velocity, but from compositional differences, that increases the P wave propagation velocity (Musacchio et al., 1997).

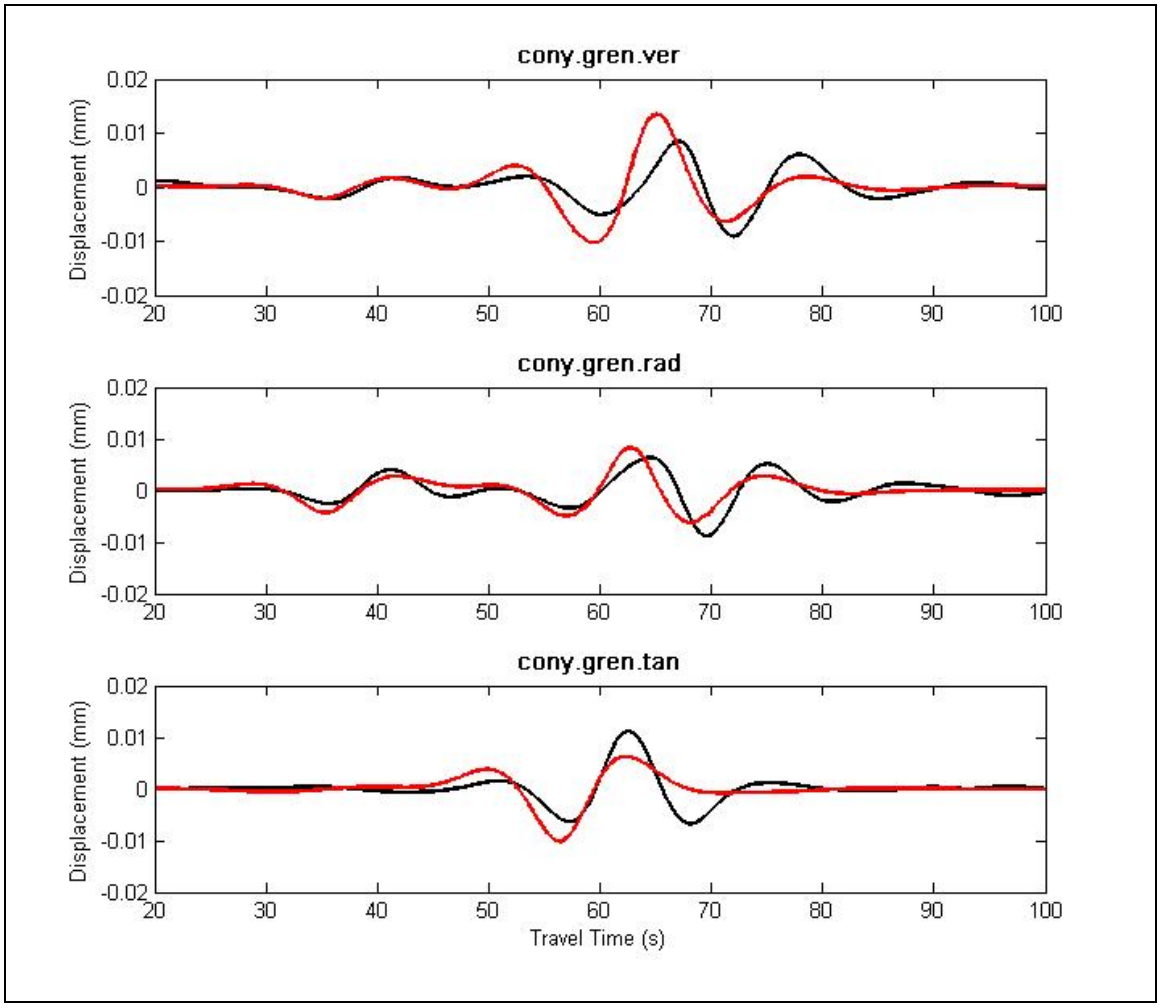

Figure 22. Recorded waveform (black line) and synthetic waveform (red line) generated with model Gren, at station CONY (Cobleskill, NY, USA), low passed below 0.1 Hz.

Like the App1 model, the Gren model works well for low frequencies (low passed at 0.1 Hz), but not as well for higher frequency content. Figure 22 illustrates the good

fitting obtained for low frequencies with model Gren at station CONY. We therefore focus on the effect of surface layers on the waveforms following the same procedure as applied to the Appalachian province. Model Gren has only a very thin (0.5 km) surface layer. We introduce more intermediate layers between the surface and the source layer (source at 11 km depth). We obtain best fits for all stations with a three layer surface gradient, with strong velocity contrasts. We designate this velocity profile by model gs3s. An example of the improved fit is shown in Figure 23 for station GAC, where the sharp contrast of the surface layer results in an increase of the late phases that better imitate the recorded waveform. As shown in Figure 23, the synthetics generated for gs3s have good timing of both P and S phases. The amplitudes are slightly high but the phasing is good. In Figure 18 we graphically depict the 1D velocity profile of model Gren and, in the inset, the change in the surface layers introduced by our new model gs3s. Plots of the synthetics resulting from the preferred model versus the data at each station in the Grenville province can be found in the Appendix.

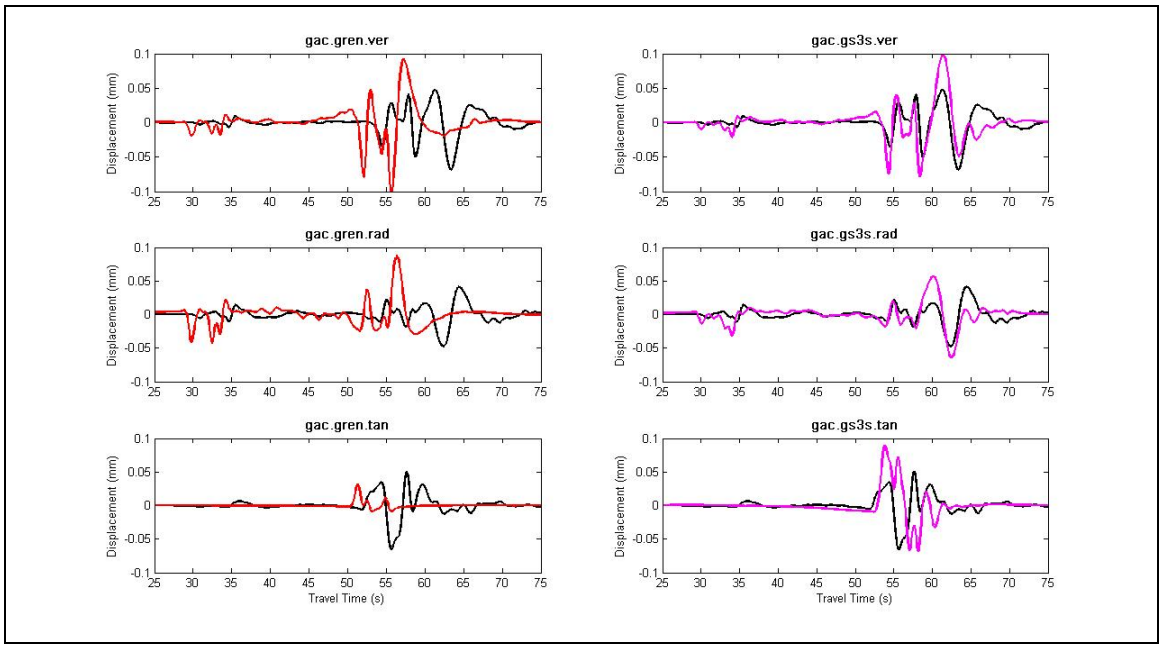

Figure 23. Three component recorded waveform at station GAC (black), synthetics generated with model gs3s (right, magenta) and synthetics generated with model Gren (left, red).

Hughes and Luetgert (1991) obtained a high velocity layer in the intermediate crust of the Grenville Province (around 17 km depth, see Figure 1), which they designated by Tahawus complex. We do not attempt to incorporate that feature in our simulations. Our results show good fits without an intermediate crustal high velocity layer.

Summary of Forward Modelling

For stations MNT and ACCN, which are over the boundary between the 2 provinces, we use the models of both provinces, and chose the one that better fits the data at each station. Because the ray paths that reach these two stations are very complex, due to the vicinity of the Champlain Thrust, we do not expect very good fits, and a 1D velocity model could be developed specifically for each station. Even so, we obtain reasonable results for station MNT with model h5 and for station ACCN with model gs3s. Table 2 indicates the preferred model for each station for both provinces.

Table 2. Preferred model for each station.

Appalachian Provinve		**Grenville Province**
Model App1 (Saikia, 1994)	**Model h5 (this study)**	**Model gs3s (this study)**
BCX	BRY	ACCN
HRV	HNH	BINY
LBNH	MNT	CONY
WES	QUA2	GAC
WVL	YLE	KGNO
		NCB

Figure 24 to 26 show the map with the locations of stations used in this study, and the recorded and synthetic waveforms computed with the preferred models, for the vertical, radial and tangential components, respectively. Synthetics generated with models gs3s are shown in red, with h5 in green, and with App1 in blue. Recorded data are displayed in black. Seismograms are filtered between 0.03 and 1 Hz. Tables with model parameters are given in the Appendix.

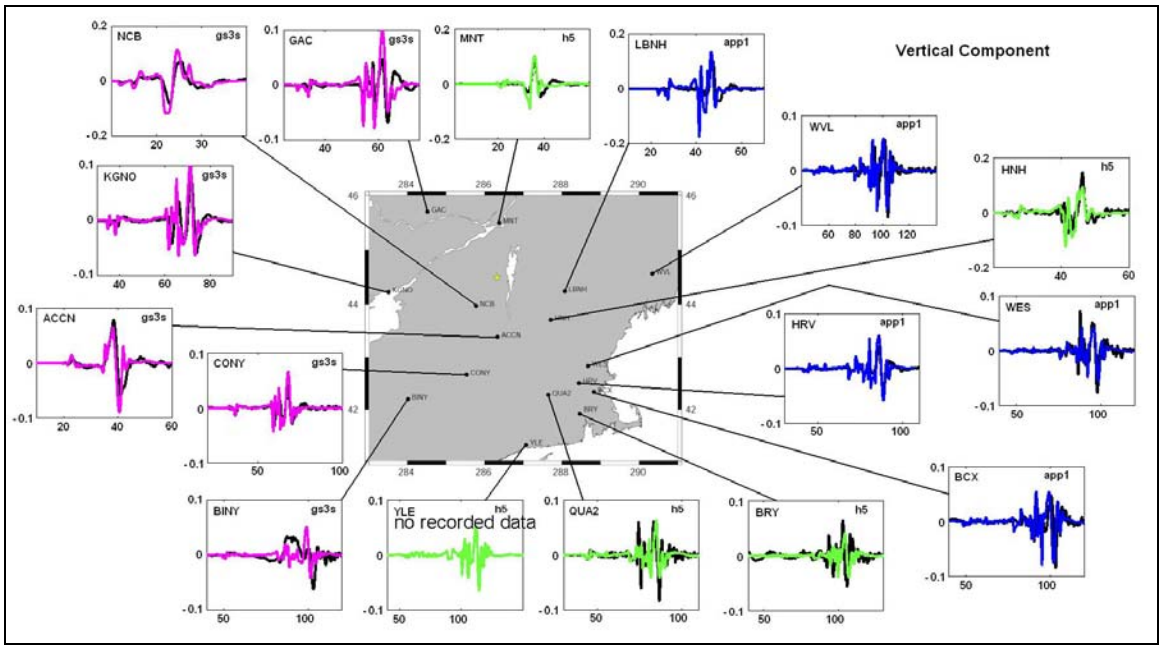

Figure 24. Map with stations used in this study, and the recorded and synthetic vertical component of the displacement seismogram computed with the preferred models. Synthetics generated with models gs3s are shown in magenta, with h5 in green, and with App1 in blue. Recorded data are displayed in black. Seismograms are filtered between 0.03 Hz and 1 Hz. Star indicates the Au Sable Fork earthquake epicenter.

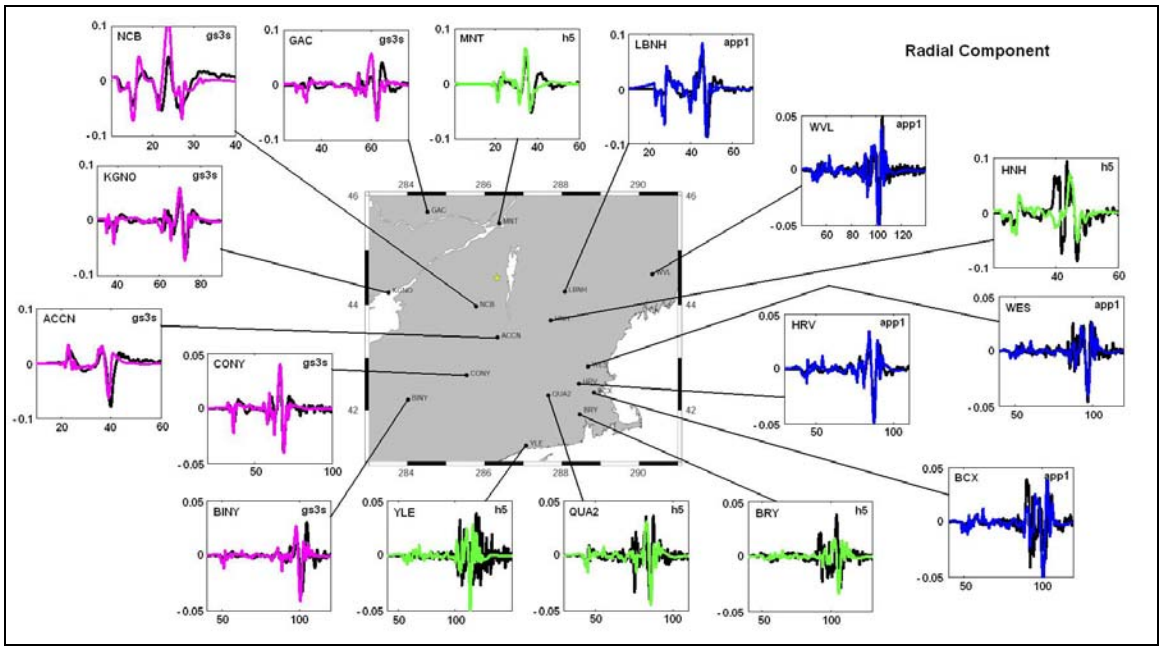

Figure 25. Same as Figure 24, but for radial component.

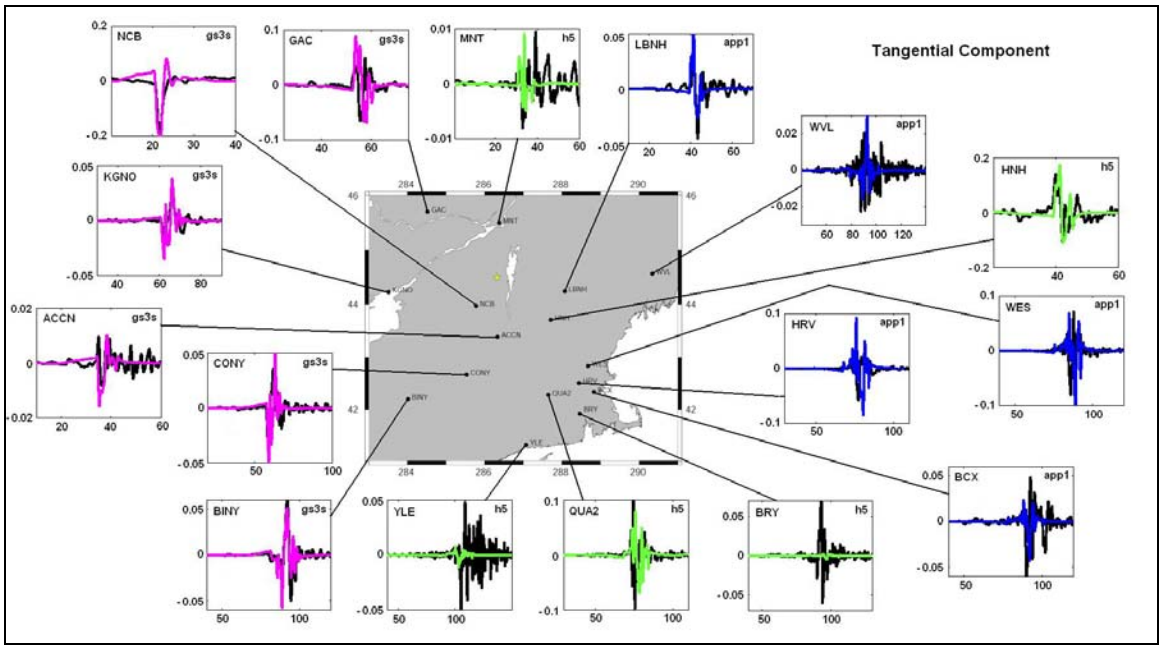

Figure 26. Same as figure 24, but for tangential component.

Discussion and Conclusions

The Au Sable Fork earthquake is the largest earthquake to be well recorded in Eastern North America. The M5.9 Saguenay earthquake in 1988 was only well recorded at one broadband stations (HRV, Harvard MA) and at several short-period stations from the Eastern Canadian Telemetered Network (ECTN) (e.g. Saikia, 1994; Zhao and Helmberger, 1991). So far, most of the regional crustal models have been developed using seismic survey data or ground motions from a single station. In the last decade, the seismic networks that operate in the region have deployed new broadband stations (around 50 or more), that recorded the Au Sable Fork earthquake. This enables us to test, validate and refine regional crustal models with a real earthquake, instead of seismic reflection/refraction data.

The relocations of the aftershocks indicate that a distinct fault plane was not evident, and therefore, the source was complex. We use the EGF method to determine an approximate source time function. We consider the 9 largest aftershocks (M3.7 to M2), which were recorded on the regional network, as potential EGFs for the mainshock (M5), but they have focal mechanisms and locations that are sufficiently different from the mainshock that we cannot resolve the mainshock source time function well. We obtain the best pulses using the largest aftershock as EGF. Due to the differences in the focal mechanisms between the mainshock and EGF, we cannot perform a slip inversion or determine the fault plane. The deconvolutions are good enough to enable us to place constraints on the shape and duration of the source pulse to use in modeling the regional waveforms. We obtain a simple triangular source pulse with an average duration of 1s, consistent with previous studies of the earthquake source parameters (e.g. Seeber et al., 2002).

We estimate an approximate static stress drop of 30 MPa, using an average corner frequency of 1 Hz. The value we obtain is consistent with high stress drops values in

stable continental regions (e.g. Kanamori, 1975). Stress drop is relevant for hazard assessment as it is directly proportional to the ground acceleration. High values thus indicate a higher damage potential.

We forward model the Au Sable Forks earthquake broadband records using the frequency-wave number method to generate synthetic seismograms. After the preliminary displacement synthetics are generated, we convolve our 1 s triangular source time function, to obtain the final synthetic seismograms. We test several published models for the Appalachian and Grenville Provinces in order to validate and choose a best-fit model for each province. We perform sensitivity tests on the best-fit model for each region (Saikia (1994) model 1 for the Appalachian Province and Hughes and Luetgert (1991) model for the Grenville Province) in order to understand the effect of crustal complexity on the waveforms. We identify differences between the recorded data and synthetics for both regions and refine the crustal models to better fit the recorded waveforms. The initial models are good at low frequencies. So, we look to improve the surface layers in the velocity models to better fit the recorded data at higher frequencies. The Appalachian Model has a detailed five layer gradient in the upper 5 km. An alternate model (model h5) with a single 3 km surface layer fit the data somewhat better at five out of ten stations in the Appalachian province. The Grenville model was very simple with only a single 0.5 km surface layer and the alternate Model gs3s with a three layer gradient in the upper 3 km shows improvements at all the stations (Figure 24 to 26).

The focus of this project was to validate and improve a 1D velocity model for both the Appalachian and Grenville Province. In the process, we have identified several potential features that could be incorporated into future 1D, 2D or 3D models of the regions. While we evaluated the effect of surface layers (upper 5 km) in both provinces and came up with best fit models for each of the stations, further iterations could be performed. Site effects are known to influence ground motions (Baise et al., 2003; Stephenson et al., 2000; Anderson et al., 1996; Borcherdt, 1970; Seed and Idriss, 1969) and more knowledge on the detailed geology at each station could improve the synthetic ground motions. In the study by Baise et al. (2003), incorporation of realistic properties for the upper 200 m of the crustal model was critical to match the simulated ground motions to the observed ground motions. In addition, incorporation of two-dimensional effects such as the Champlain Thrust at the intersection of the Appalachian and Grenville provinces and other geologic complexities such as directivity or anisotropy (Hughes et al., 1993) could improve the synthetic waveforms. Future work should identify and incorporate the possible anisotropy in the crust that is evident at HRV and other nearby stations in the Appalachian province.

Acknowledgments

This research is sponsored by USGS External Grant Award Number 04HQGR0166 and 04HQGR0167.

Data was retrieved from IRIS (Incorporated Research Institutions for Seismology), CNSN (Canadian National Seismograph Network) and Weston Observatory.

Publications:

Viegas, G., Abercrombie, R., Baise, L. and Kim, W. (2005). Earthquake source scaling and wave propagation in eastern North America: the Au Sable Forks, NY, earthquake, *EOS, Trans, AGU,* 86(52), Fall Meeting Suppl., Abstract S23B-0247.

References

Abercrombie, R.E. and Rice, J.R. (2005). Small Earthquake scaling revisited: can it constrain slip weakening?, *Geophys. J. Int.*, **162**, 406-424.

Anderson J.G., Lee, Y., Zeng, Y. and Day, S. (1996). Control of strong motion by the upper 30 meters, *Bull. Seism. Soc. Am.,* **86**(6), 1749-1759.

Atkinson G.M. and Boore, D.M. (1995). Ground-motion relations for eastern North America, *Bull. Seism. Soc. Am.* **85**(1), 17-30.

Atkinson G.M. and Boore, D.M. (1998). Evaluation of models for earthquake source spectra in eastern North America, *Bull. Seism. Soc. Am.* **88**(4), 917-934.

Atkinson G.M. and Sonley, E. (2003). Ground motions from the 2002 Au Sable Forks, New York earthquake of M5.0, *Seism. Res. Lett.*, **74**(3), 339-349.

Baise, L., Dreger, D.S. and Glaser, S. (2003). The Effect of Shallow San Francisco Bay Sediments on Waveforms Recorded during the M_W 4.6 Bolinas, California, Earthquake, *Bull. Seism. Soc. Am.* **93**(1), 465-479.

Borcherdt, R.D. (1970). Effects of local geology on ground motion near San Francisco Bay, *Bull. Seism. Soc. Am.*, **60**, 29-61.

Campbell, K. (2003) Prediction of strong ground motion using the hybrid empirical method and its use in the development of ground-motion (attenuation) relations in Eastern North America. *Bull. Seism. Soc. Am.* **93**(3), 1012-1033.

Detweiler, S. and Mooney, W.D. (2002). The Relation of the Grenville/Appalachian Boundary to the April 20, 2002 Au Sable Forks, New York and the April 29, 2003 Fort Payne, Alabama Earthquakes. *EOS, Trans, AGU,* **84**(46), Fall Meeting Suppl., Abstract S21E-0348.

Du, W.-X., Kim, W.-Y. and Sykes, L.R. (2003). Earthquake source parameters and state of stress for the northeastern United States and southeastern Canada from analysis of regional seismograms, *Bull. Seism. Soc. Am.*, **93**(4):1633-1648.

Eaton, D.W., Dineva, S. and Mereu, R. (2006). Crustal thickness and Vp/Vs variations in the Grenville orogen (Ontario, Canada) from analysis of teleseismic receiver functions. *Tectonophysics*, **420**, 223-238.

Eshelby, J.D. (1957). The determination of the elastic field of an ellipsoidal inclusion and related problems, *Proc. R. Soc. London A.*, **241**, 376-396.

Frankel, A., A. McGarr, J. Bicknell, J. Mori, L. Seeber, and E. Cranswick (1990), Attenuation of high-frequency shear waves in the crust: Measurements from New York State, South Africa, and Southern California, *J. Geophys. Res.*, **95**(B11), 17441–17457.

Hartzell, S.H. (1978). Earthquake aftershocks as Green's functions, *Geophys. Res. Letters*, **5**, 1-4.

Hughes S, and Luetgert, J.H. (1991). Crustal structure of the western New England Appalachians and the Adirondack Mountains *J. Geophys. Res*., **96**, 16471-16494.

Hughes S, and Luetgert, J.H. (1992). Crustal structure of the southeastern Grenville province, northern New York and Eastern Ontario, *J. Geophys. Res*., **97**, 17455-17479.

Hughes,S., Luetgert, J. H. and Christensen, N. I. (1993). Reconciling deep seismic refraction and reflection data from the Grenvillian-Appalachian boundary in western New England, *Tectonophysics*, **225**(4), 255-269.

Kanamori, H. and Anderson, D.L. (1975). Theoretical basis of some empirical relations in seismology, *Bull. Seismol. Soc. Am.*, **65**(5), 1073-1095.

Kim, W.-Y. and Abercrombie, R.E. (2006). Source scaling of earthquakes in the northeastern united states: Collaborative research with Columbia University and Boston University, *NEHRP Final Technical Report*, Award Number: 04HQGR-0028.

Ma, S. and Atkinson, G.M. (2006). Focal depths for small to moderate earthquakes (mN≥2.8) in Western Quebec, Southern Ontario, and Northern New York, *Bull. Seism. Soc. Am.*, **96**(2), 609-623.

Madariaga, R. (1976). Dynamics of an expanding circular crack, *Bull. Seismol. Soc. Am.*, **66**, 639-666.

Mareschal, J.C. and Jaupart, C. (2004). Variations of surface heat flow and lithospheric thermal structure beneath the North American craton, *Earth and Plan. Sci. Letters*, **223**, 65-77.

Musacchio, G., Mooney, W.D., Luetgert, J.H. and Christensen, N.I. (1997). Composition of the crust in the Grenville and Appalachian Provinces of North America inferred from VP/VS ratios, *J. Geophys. Res.*, **102**, 15225-15242.

Saikia, C.K. (1994). Modified Frequency-Wavenumber Algorithm for Regional Seismograms using Filon's Quadrature: Modelling of Lg Waves in Eastern North America. *Geophys. J. Int*., **118**, 142-158.

Seeber, L., Kim, W.-Y., Armbruster, J.G., Du, W.-X., and Lerner-Lam, A. (2002). The 20 April 2002 Mw 5.0 earthquake near Au Sable Forks, Adirondacks, New York: A first glance at a new sequence, *Seis. Res. Lett.*, **73**, 480-489.

Seed, H.B. and Idriss, I.M. (1969). The influence of soil conditions on ground motions during earthquakes. *J. Soil Mech. Found. Div. ASCE*, **94**, 93-137.

Shi J., Kim, W.-Y. and Richards, P.G. (1996). Variability of crustal attenuation in the northeastern United States from Lg waves, *J. Geophys. Res*., **101**, 25231-25242.

Somerville, P. (1989). Earthquake Source and Ground-Motion Characteristics in Eastern North America, *Annals New York Academy of Sciences*, **558**, 105-127.

Stephenson, W.J., Williams, R.A., Odum, J.K. and Worley, D.M. (2000). High-resolution seismic reflection surveys and modeling across an area of high damage from the 1994 Northridge earthquake, Sherman Oaks, California, *Bull. Seism. Soc. Am.*, **90**(3), 643-654.

Taylor, S.R., Toksoz, M.N. and Chaplin, M.P. (1980). Crustal structure of the northeastern United States: contrasts between Grenville and Appalachian Provinces, *Science*, **208**, 595-597.

Toro, G., Abrahamson, N. and Schneider, J. (1997). Model of strong motion in Eastern and Central north America: Best estimates and uncertainties, *Seism. Res. Lett.*, **68**, 41-57.

Viegas, G., Abercrombie, R., Baise, L. and Kim, W. (2005). Earthquake source scaling and wave propagation in eastern North America: the Au Sable Forks, NY, earthquake, *EOS, Trans, AGU*, **86**(52), Fall Meeting Suppl., Abstract S23B-0247.

USGS Earthquake Hazards Program: Earthquake Report: New York. (2002) *Magnitude 5.2 NEW YORK 2002 April 20 10:50:47 UTC, Preliminary Earthquake Report* http://neic.usgs.gov/neis/eq_depot/2002/eq_020420/

Wheeler, R.L. (1995). Earthquakes and the cratonward limit of Iapetan faulting in eastern North America, *Geology*, **23**, 105-108.

Zhao, L.S. and Helmberger, D.V. (1991). Broad-band modeling along a regional shield path, Harvard recording of the Sanguenay earthquake, *Geophys. J. Int.*, 105(2), 301-312.

Zhu and Ebel, 1994. Tomographic inversion for the seismic velocity structure beneath northern New England using seismic refraction data, *J. Geophys. Res*., **99**, 15331-15357.

Appendix

Model App1

Thickness (km)	Vp (km/s)	Vs (km/s)	Density (kg/m3)	Qp	Qs
1.00	5.600	3.240	2.820	500	250
1.00	5.732	3.310	2.846	500	250
1.00	5.864	3.350	2.873	500	250
1.00	5.996	3.470	2.899	500	250
1.00	6.128	3.550	2.926	500	250
3.00	6.260	3.620	2.952	500	250
8.00	6.450	3.670	2.990	1000	500
8.00	6.590	3.750	3.020	1000	500
11.00	6.710	3.820	3.040	8600	6200
10.00	8.100	4.600	3.320	8600	6200
10.00	8.350	4.700	3.370	8600	6200
10.00	8.400	4.755	3.380	8600	6200
10.00	8.410	4.775	3.387	8600	6200
10.00	8.420	4.794	3.393	8600	6200
10.00	8.421	4.813	3.400	8600	6200
10.00	8.422	4.833	3.407	8600	6200
10.00	8.425	4.852	3.413	8600	6200
10.00	8.430	4.871	3.420	8600	6200

Model h5

Thickness (km)	Vp (km/s)	Vs (km/s)	Density (kg/m3)	Qp	Qs
3.00	5.732	3.310	2.846	500	250
13.00	6.450	3.670	2.990	1000	500
8.00	6.590	3.750	3.020	1000	500
11.00	6.710	3.820	3.040	8600	6200
10.00	8.100	4.600	3.320	8600	6200
10.00	8.350	4.700	3.370	8600	6200
10.00	8.400	4.755	3.380	8600	6200
10.00	8.410	4.775	3.387	8600	6200
10.00	8.420	4.794	3.393	8600	6200
10.00	8.421	4.813	3.400	8600	6200
10.00	8.422	4.833	3.407	8600	6200
10.00	8.425	4.852	3.413	8600	6200
10.00	8.430	4.871	3.420	8600	6200

Model gs3s

Thickness (km)	Vp (km/s)	Vs (km/s)	Density (kg/m3)	Qp	Qs
1.00	5.600	3.127	2.820	600	300
1.00	5.900	3.301	2.890	600	300
1.00	6.200	3.475	2.900	600	300
15.00	6.600	3.668	2.900	600	300
22.00	6.900	3.861	2.900	1000	500
40.00	8.100	4.440	3.300	8600	6200

Preferred Models

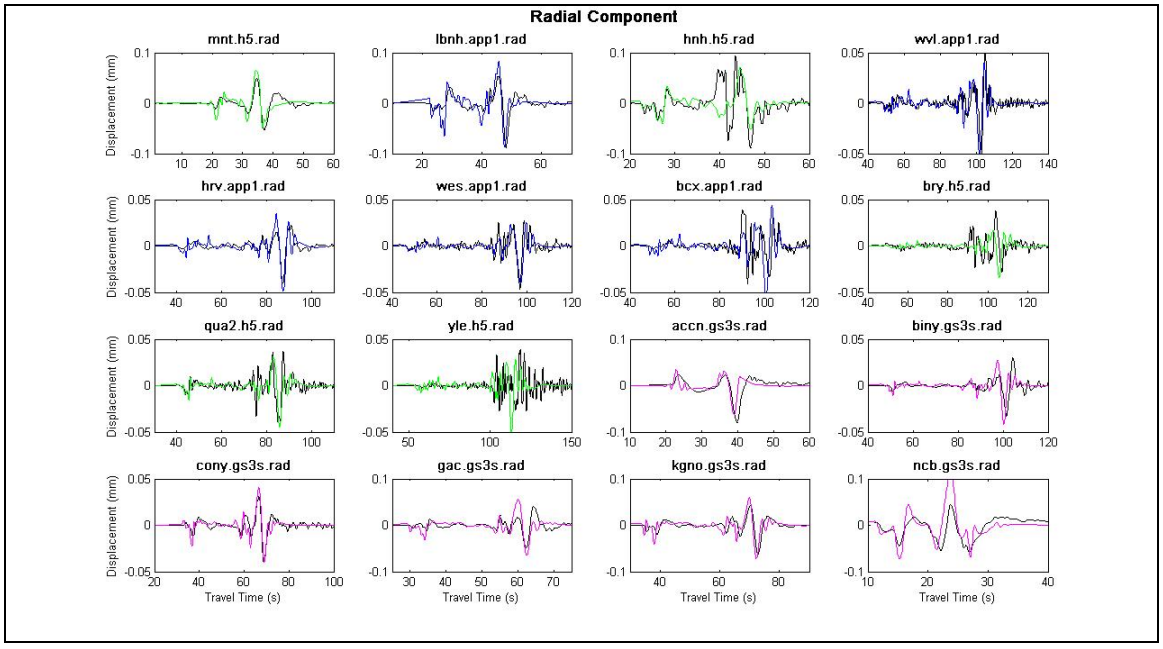

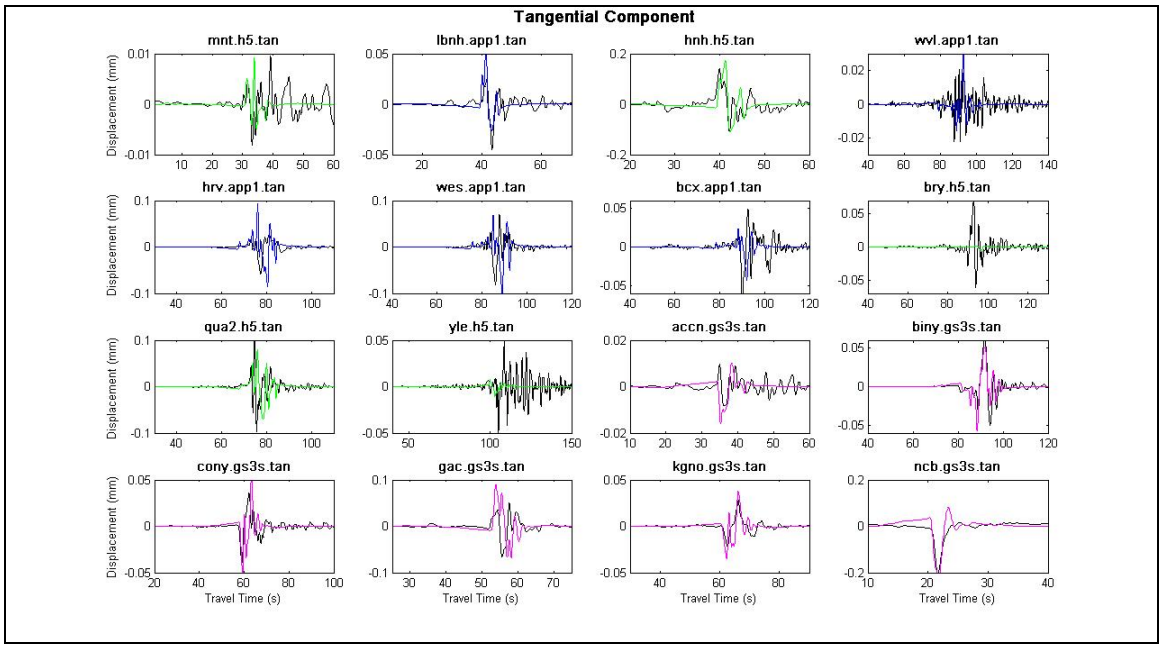
Tangential Component
mnt.h5.tan
lbnh.app1.tan
hnh.h5.tan
wvl.app1.tan
hrv.app1.tan
wes.app1.tan
bcx.app1.tan
bry.h5.tan
qua2.h5.tan
yle.h5.tan
accn.gs3s.tan
biny.gs3s.tan
cony.gs3s.tan
gac.gs3s.tan
kgno.gs3s.tan
ncb.gs3s.tan
Displacement (mm)
Travel Time (s)

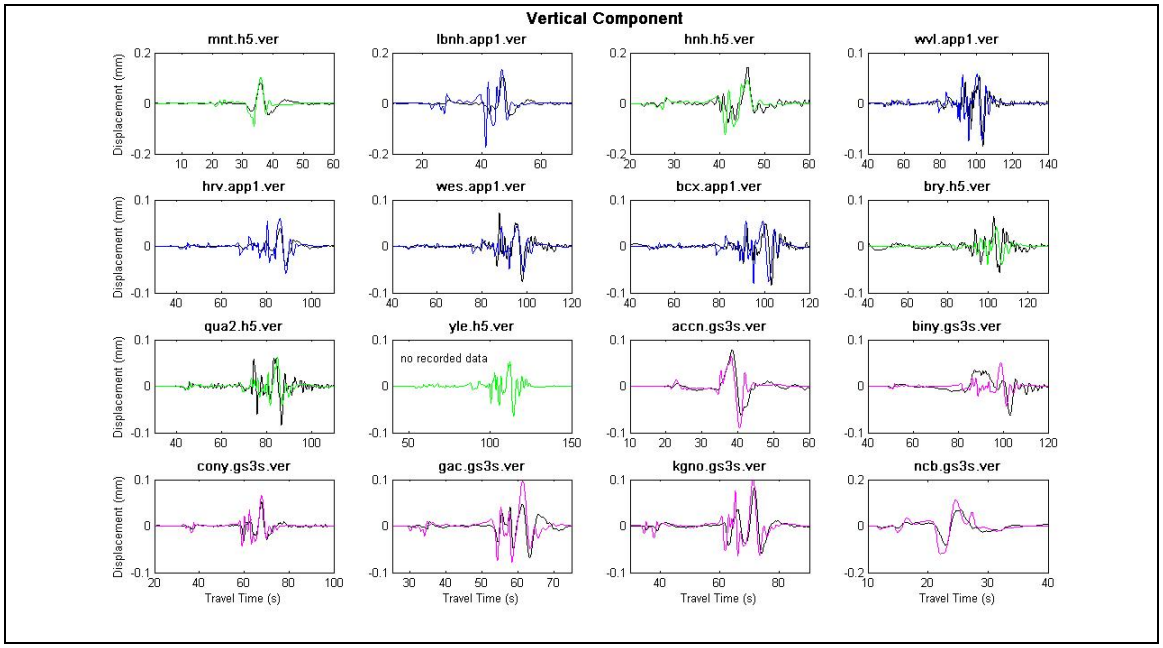
Vertical Component
mnt.h5.ver
lbnh.app1.ver
hnh.h5.ver
wvl.app1.ver
hrv.app1.ver
wes.app1.ver
bcx.app1.ver
bry.h5.ver
qua2.h5.ver
yle.h5.ver
no recorded data
accn.gs3s.ver
biny.gs3s.ver
cony.gs3s.ver
gac.gs3s.ver
kgno.gs3s.ver
ncb.gs3s.ver
Displacement (mm)
Travel Time (s)